DESIGN ANALYSIS OF A SLAG POT TRANSFER CAR

A Thesis Submitted in Partial Fulfillment of The Requirements for Awarding the Degree Of

Master of Automobile Engineering
Faculty of Engineering and Technology

Submitted by

RAVI NISHAD
Registration No.- 163716 of 2022-24
Examination Roll No.- M4AUT24001

Under the guidance of

Prof. Dipankar Sanyal,

Department of Mechanical Engineering Jadavpur University

Mr. Syed Abdus Shahid,
Primetals Technologies India Pvt. Limited

DEPARTMENT OF MECHANICAL ENGINEERING
JADAVPUR UNIVERSITY
KOLKATA -700032
INDIA

2024

FACULTY OF ENGINEERING AND TECHNOLOGY
DEPARTMENT OF MECHANICAL ENGINEERING
JADAVPUR UNIVERSITY
KOLKATA

DECLARATION OF ORIGINALITY
AND
COMPLIANCE OF ACADEMIC ETHICS

I hereby declare that this thesis contains a literature survey and original research work by the undersigned candidate as part of his ***Master of Engineering*** *studies.*
All information in this document has been obtained and presented in accordance with academic rules and ethical conduct.
I also declare that, as required by these rules and conduct, I have fully cited and referenced all materials and results that are not original to this work.

Name : **Ravi Nishad**
Examination Roll No : **M4AUT24001**
Thesis Title : **Design Analysis of a Slag Pot Transfer Car**.

Signature :
Date :

FACULTY OF ENGINEERING AND TECHNOLOGY
DEPARTMENT OF MECHANICAL ENGINEERING
JADAVPUR UNIVERSITY
KOLKATA

CERTIFICATE OF RECOMMENDATION

We hereby recommend that this thesis under our supervision by **Ravi Nishad**, entitled, **"Design Analysis of a Slag Pot Transfer Car"** be accepted in partial fulfilments for awarding the degree of Master of Engineering under Department of Mechanical Engineering of Jadavpur University.

……..

Prof. Dipankar Sanyal

Thesis Advisor

Dept. of Mechanical Engineering

Jadavpur University,Kolkata

……..

Prof. Swarnendu Sen

Head of Department

Dept. of Mechanical Engineering

Jadavpur University,Kolkata

……..

Prof. Dipak Laha

DEAN

Faculty of Engineering & Technology

Jadavpur University,Kolkata

FACULTY OF ENGINEERING AND TECHNOLOGY
DEPARTMENT OF MECHANICAL ENGINEERING
JADAVPUR UNIVERSITY
KOLKATA

CERTIFICATE OF APPROVAL

The foregoing thesis entitled "**Design Analysis of a Slag Pot Transfer Car"** is hereby approved as a creditable study of an engineering subject carried out and presented in a manner satisfactory to warrant its acceptance as a prerequisite to the degree for which it has been submitted. It is notified to be understood that by this approval, the undersigned do not necessarily endorse or approve any statement made, opinion expressed and conclusion drawn therein but approve the thesis only for the purpose for which it has been submitted.

Committee of final examination for evaluation of thesis;

…… …….

…… …….

…….
……...

Signature of Examiners

Acknowledgement

First and foremost, I extend my deepest gratitude to my supervisor, Prof. Dipankar Sanyal, Professor, Department of Mechanical Engineering, Jadavpur University,
Mr. Santosh Mohapatra, HoD, EN-SM, Mr. Kinsuk Bandyopadhyay, Executive Vice President and Mr. Syed Abdus Shahid, Senior Manager, Design, Primetals Technologies India Pvt. Limited, for his unwavering inspiration, motivation, and invaluable advice throughout my project. He guided me in the right direction to pinpoint my areas of strength and provided me with the psychological and informational support, academics, and personal guidance throughout the work. I am truly grateful to him for helping me reach this goal and for keeping me on the right path.

I would like to express my gratitude to Mr. Mr. Syed Abdus Shahid, a Design Senior Manager who is my internship advisor, for his invaluable guidance on some aspects of this thesis. When I went to him with a new problem involving my work, he always offered the best solutions. The ability to prepare this thesis was greatly aided by his insightful and priceless advice.
I am very grateful for this opportunity and look forward to continuing my work.

Dept. of Mechanical Engineering
Jadavpur University, Kolkata, India

[RAVI NISHAD]

ABSTRACT

This thesis aims to development and performance analysis of the main frame with cost and material optimization, using materials E250BR with high strength. This abstract presents a novel approach to the design of the frame for slag pot transfer cars, aimed at enhancing efficiency, durability, and safety in industrial operations. The proposed design integrates advanced materials, structural optimization techniques, and innovative features to address the challenges faced in conventional design.The new frame design incorporates lightweight yet high-strength materials, such as advanced alloys or composites, to reduce the overall weight of the transfer car without compromising structural integrity. This not only improves energy efficiency but also allows for increased payload capacity and operational flexibility.

Structural optimization techniques, including finite element analysis (FEA) are employed to optimize the distribution of material within the frame, resulting in an optimized design that minimizes stress concentrations and maximizes load-bearing capacity. This ensures robust performance under varying operating conditions and extends the service life of the transfer car.

In addition to structural improvements, the new frame design integrates advanced safety features such as collision detection systems, emergency braking mechanisms, and real-time monitoring capabilities. These features enhance workplace safety and reduce the risk of accidents, contributing to a safer working environment.

Overall, the proposed design offers significant advancements over traditional frame designs for slag pot transfer cars, promising improved efficiency, durability, and safety in industrial material handling operations. Future work will focus on prototype development and validation through rigorous testing and real-world deployment.

For the Analysis of whole frame in NX 2212 advance simulation version is used to perform this analysis and Solid Edge software is used for design and 3D modelling the frame. And AutoCad is used for 2 D drawing and making geometry of components.

NOMENCLATURE

b	*Width*
d	*Depth*
X, Y	*Dimensionless coordinates*
G	*Centre of gravity*
$\bar{y}$	*Distance of a point from neutral axis*
A	*Area*
Y_g	*Coordinate of the centre of mass*
I_{XX}	*Centroidal X axis*
I_{YY}	*Centroidal Y axis*
I	*Moment of Inertia*
σ	*Bending stress*
M	*Bending moment*
E	*Young modulus*
R_C	*Radius of curvature*
σ_{max}	*Maximum bending stress*
Z	*Section modulus*
R	*Support reaction*
W	*Transverse Load*
L	*Length*
Y_c	*Deflection*
m	*Mass*
R_{eH}	*Minimum yield stress*
t	*Plate thickness*
a_t	*Centre to centre track distance*
a_w	*Centre to centre wheel distance*
d	*Bore diameter of bearing*
D	*Outside diameter of bearing*
a	*Acceleration*
F_x	*Spring force*
s	*Stifness of spring*
v	*Velocity*
Gr	*Dead load of slag pot car*
Gsp	*Dead load of full slag pot*
Fx	*Force in x-direction*
Fy	*Force in y-direction*
Fz	*Force in z-direction*
f_y	*Yield point*
γ_m	*General resistance factor of the plate*
γ_{sm}	*Specific resistance factor of the plate*
f_{Rd}	*Limit design stress*

LIST OF FIGURES

TABLE OF CONTENT

Contents

CHAPTER 1: INTRODUCTION

1.1 Slag and Slag-Pot Transfer Car

Slag is metallurgical waste. In the context of metal smelting or refining, it is the stony leftover of the extraction process for metals from their ores. During iron or steel production, slag forms as a by-product when impurities are removed from the molten metal. This slag is usually discarded.

A slag pot transfer car, also known as a slag pot carrier or slag pot transporter, is a specialized piece ofequipment used in metallurgical plants, particularly in steelmaking facilities.

When molten metal is produced in a blast furnace or during steelmaking processes, impurities called slag are formed. Slag is a byproduct consisting of various non-metallic compounds that float on top of the molten metal. It needs to be removed to ensure the quality of the final product.

The weight makes manual handling impractical and dangerous. Hence, large containers called slag pots are used to collect and transport slag away from the production area. These pots can be extremely heavy, when filled with molten slag.

A slag pot transfer car is essentially a heavy-duty, rail-mounted vehicle designed to transport slag potswithin the plant. These cars are equipped with specialized mechanisms to securely lift and move the heavy slag pots from one location to another. They are often automated or semi-automated to ensure efficiency and safety in the transportation process.

Overall, slag pot transfer cars play a crucial role in the efficient operation of metallurgical plants by facilitating the safe handling and transportation of slag, helping to streamline the production process and maintain a clean and safe working environment.

1.2 Usefulness of Slag Pot Transfer Car

Slag pot transfer cars serve several important purposes, as listed next.

1. **Slag Removal:** One of the primary functions of slag pot transfer cars is to remove slag from theproduction area. After molten metal is tapped from a furnace, slag forms on the surface. The transfer car is used to transport empty slag pots to the tapping area and then carry away the filled potscontaining the molten slag.
2. **Transportation**: Slag pots, when filled, can be extremely heavy and cumbersome to move manually. Slag pot transfer cars are designed to safely lift and transport these heavy pots within the plant premises. By using rail-mounted transfer cars, the transportation process becomes more efficientand less labor-intensive.
3. **Safety:** Handling molten slag is hazardous due to its high temperature and chemical composition. Slag pot transfer cars provide a safer alternative to manual handling by reducing the risk of accidentsand injuries associated with moving heavy loads of molten slag.
4. **Efficiency:** The use of transfer cars streamlines the slag removal process, allowing for faster turnaround times between production cycles. This efficiency is crucial in maintaining the overallproductivity of the plant.

5. **Automation:** Many modern slags pot transfer cars are equipped with automation features, such as programmable controls and sensors, which enable precise positioning and movement of the slag pots. Automation increases operational efficiency and reduces the reliance on manual labor.
6. **Maintenance:** Transfer cars also play a role in maintenance activities within the plant. They can beused to transport slag pots to designated maintenance areas for inspection, repair, or cleaning, ensuring the longevity and proper functioning of the equipment.

In summary, the use of slag pot transfer cars optimizes the handling and transportation of molten slag in metallurgical plants, contributing to increased safety, efficiency, and productivity. These cars have immense scope of applications in steelmaking operations in India.

1.3 Steel Production in India and Abroad

According to the Indian Steel Association, India had a total installed steel-making capacity of 154 million tonnes (MT) as of March 2023. India also surpassed Japan as the second largest steel producer in the world in 2018, with a crude steel production of 106.5 MT.

Some of the major steel plants in India are:

- SAIL Steel Plant at Bokaro Steel City, Jharkhand - the second biggest steel plant in India, which contributes 45% of SAIL's profit.
- JSW Steel at Hospet, Bellary, Karnataka - the largest private sector steel producer in India, with a capacity of 18 MT
- Jindal Steel and Power Limited at Raigarh, Chhattisgarh - the third largest steel producer inIndia, with a capacity of 8.6 MT.
- RINL - Visakhapatnam Steel Plant at Visakhapatnam, Andhra Pradesh - a Navaratna PSE under the Ministry of Steel, with a capacity of 7.3 MT.

Steel has been a material of choice for innumerable applications all along in the past, and it is likely to continue to be an important material for use in the foreseeable future. The world steel production hasbeen increasing from year to year and has already crossed the 1 billion tones mark for the first time in 2004. During the intervening period, steel production has grown very fast, and in 2010, global steel production has exceeded 1.4 billion tones. The rapid increase has been led by China accounting for more than 45% of world steel production. China is not only the largest producer of steel (627 million tons), but it is also the largest consumer of steel (576 million tonnes) followed by the United States and India. An analysis of the Technology Profile of World Steel Industry shows that 70% steel is produced through the Basic Oxygen Furnace (BOF)/LD Convertor route, 28.8% through Electric Steel Making route and the balance 1.2% through the open hearth (OH). The open-hearth route of productionis almost extinct from the world map except in some of the countries like Russia and Ukraine [1].

1.4 Production of Steel

Steel is produced from iron ore or scrap metal in industrial facilities called plants. Two main types of steel plants in India are integrated and mini types.

Integrated steel plants carry out all the steps of steelmaking, from smelting iron ore to rolling finished products. Mini steel plants use electric arc furnaces to melt scrap metal and produce steel.

The production of steel requires several steps, as depicted in Figure 1.1. Different processes are executed in.

1. Blast Furnace shown in Figure 1.2
2. Steelmaking furnaces that could be
   - Basic Oxygen Furnace (BOF) depicted in Figure 1.3
   - Electric Arc Furnace shown in Figure 1.4
3. Ladle refining, casting and finishing strands to carry out
   - Casting
   - Rolling and Forming
   - Finishing

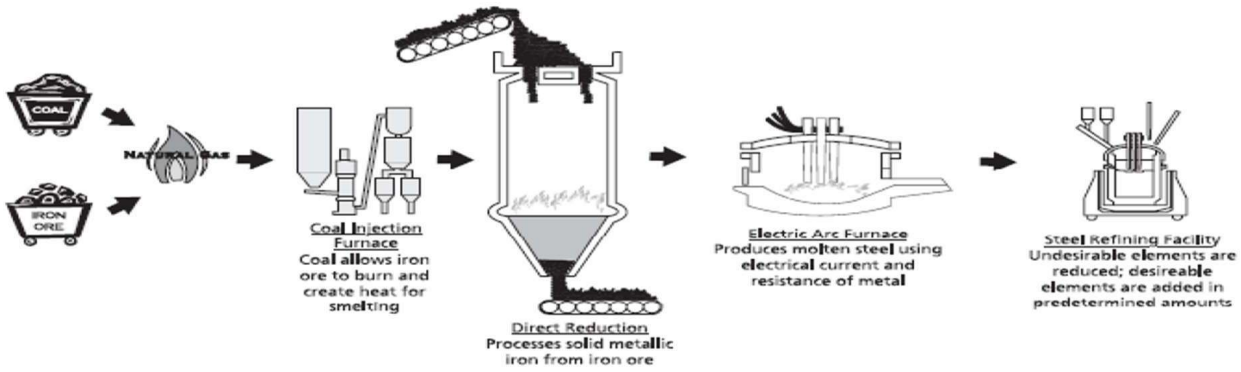

Figure 1.1 Steelmaking process [2]

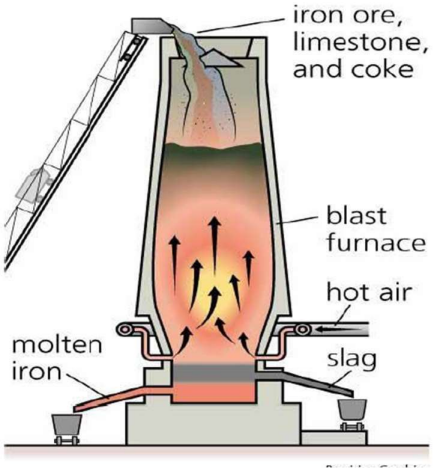

Figure 1.2 Blast Furnace [2]

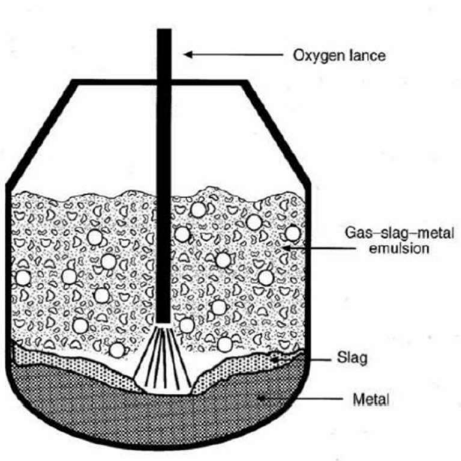

Figure 1.3 Basic Oxygen Furnace (BOF) [2]

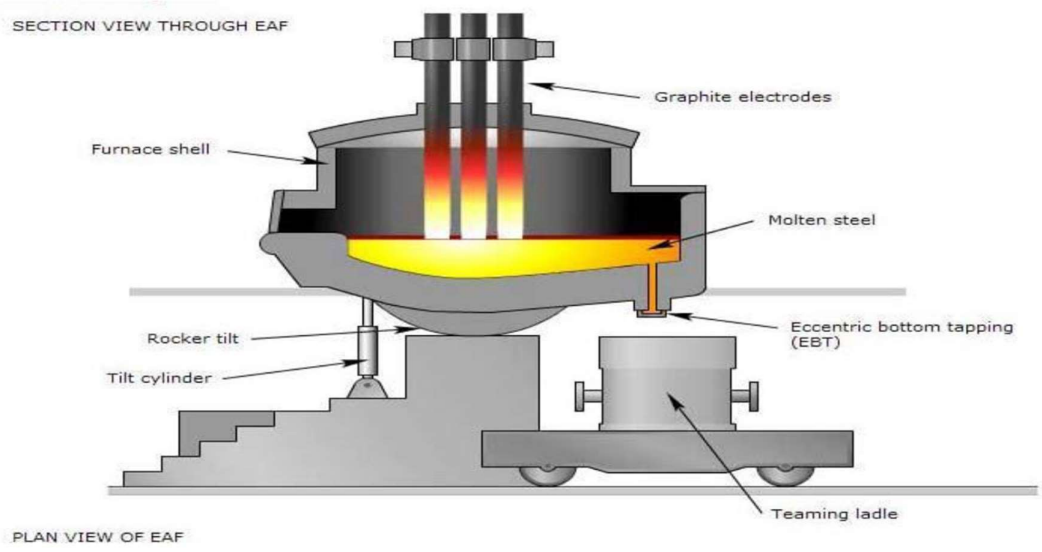

Figure 1.4: Electric Arc Furnace [2]

Visakhapatnam Steel Plant (VSP) is bestowed with modern technologies. It has an installed capacity of 3 million tons per annum of liquid steel and 2.656 million tons of saleable steel. At VSP, there is an emphasis on total automation, seamless integration and efficient upgradation that results in wide range of long and structural products to meet stringent demands of discerning customers within India and abroad. VSP products meet exacting international quality standards such as JIS, DIN, BIS, and BS. VSP has become the first integrated steel plant in the country to be certifiedto all three international standards for quality (ISO-9001), for environment management (ISO 14001) and for occupational health and safety (OHSAS-18001). This covers quality systems of all operational, maintenance, and service units besides purchase systems, training and marketing functions spreading over four regional marketing offices, 24 branch offices, and stockyards located all over the country.
Of course, more optimization is necessary for the effective usage of transport of the slagin steel industries. This is to minimize the material handling cost and manhandling of production. Time of handlingis should also be minimized so as to maximize the quantity of production.

1.5 Existing Slag Pot Transfer Cars

Most of the existing transfer cars shown in Figures 1.5 and 1.6 are propelled on four wheels receiving torque from four motors. Some of their drawbacks are their bulk and manual operation. Tilting ladle transfer cars are used to carry hot metal ladles from the HMDS plant to the convertor section. The molten metal consists of slag and impurities, which affect the purity of the final metal. The ladle carries the hot metal in a car. From removing the slag by raking machine, the ladle is tilted. Steel is an alloy consisting of iron, with a carbon content of between 0.02% and 2% by weight, and small amounts of alloying elements, such as manganese, molybdenum, chromium, or nickel. Steel has a wide range of properties that are largely determined by chemical composition (carbon and other alloys), controlled heating and cooling applied to it, and mechanical “working” of the steel in the finishing process .

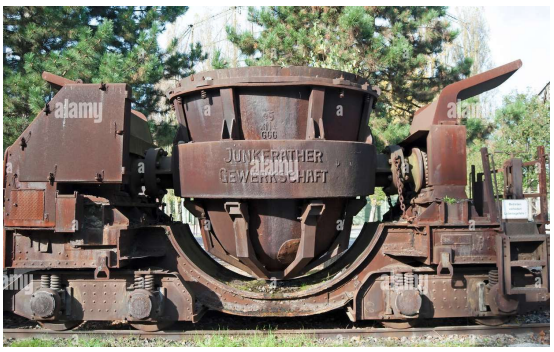

Figure 1.5: Existing bulky slag-pot car [3] **Figure 1.6: Manually operated slag-pot car [4]**

The shortcomings of old slag pot transfer cars are as follows.

- Bulky
- Integrated tilter.
- Capable of dumping in nearby area
- Imprecise control
- Manual tilting
- 4-wheel drive consuming high power.
- Overheating of drive unit
- Traditional design without specific modifications to address issues like powercable damage due to high temperature slag.
- Poor safety and efficiency

1.6 Proposed Improvements in the Present Design

Slag pot transportation car is one of the steel metallurgical special vehicles. A design methodology has been developed that has been employed to design a car for a foundry industry having a distance of 84650mm between the converter sections and the slag yard. The proposed design aims to replace the existing crane arrangement for transporting the molten slag. Salient points of the proposed design are.

- Safety and efficient design based on fundamental theory and emerging techniques like finite element method and electrical measurement experiments to determine the critical points and sections in the frame.
- New generation slag pot transfer car incorporating better features in the vertical structure called mast.
- High strength to raise the loading capacity.
- Use of slag-scraper to clean the track.
- Two-wheel drive
- Drive unit cover with better ventilation.
- Eliminating the possibility of damage to power cables caused by slag leakage or spillage.
- Reduced material handling cost.

1.7 Overview of Computer-Aided design Model of slag pot transfer car

A computer-aided design, or CAD, model is prepared in **Solid Edge software** for a slag pot transfer car. Figures 1.7 to 1.13 show different views of the proposed design with appropriate title for each figure.

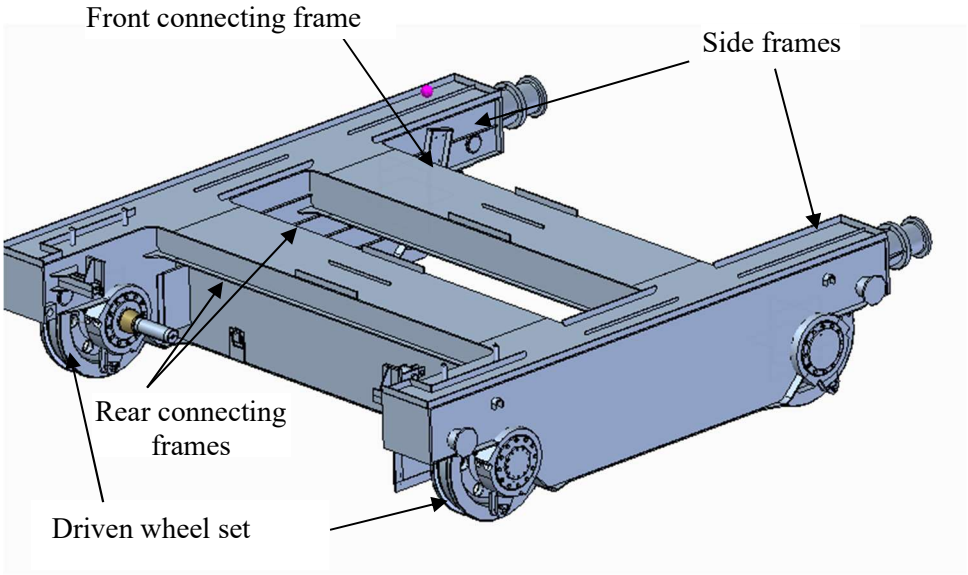

Figure 1.7: CAD Model of main frame with driven wheel set labelled.

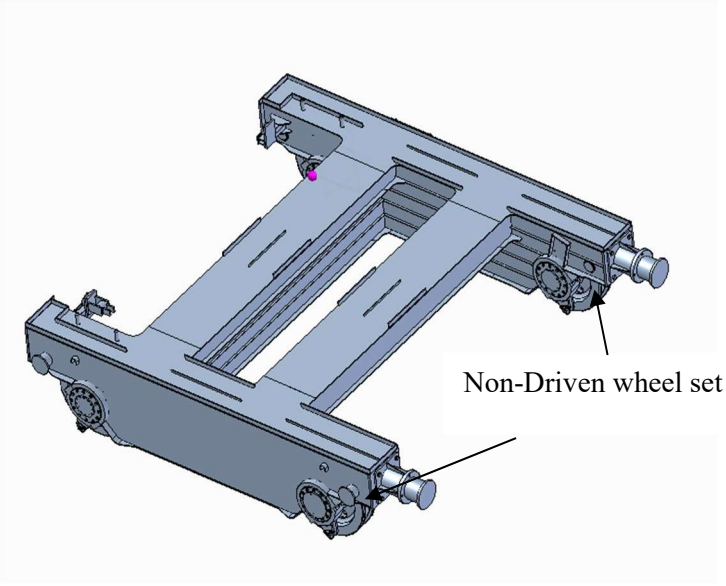

Figure 1.8: CAD Model of main frame with the set of non-driven wheels labelled.

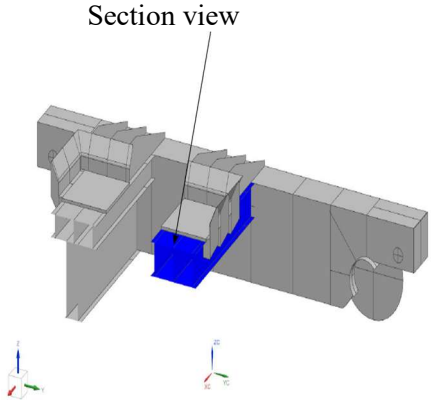

Figure 1.9: Sectional view of the front connecting frame.

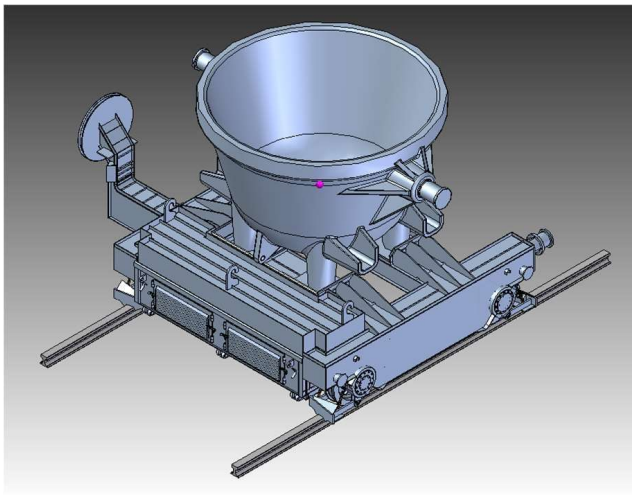

Figure 1.10: Full assembly of proposed design with slag pot mounted on the car

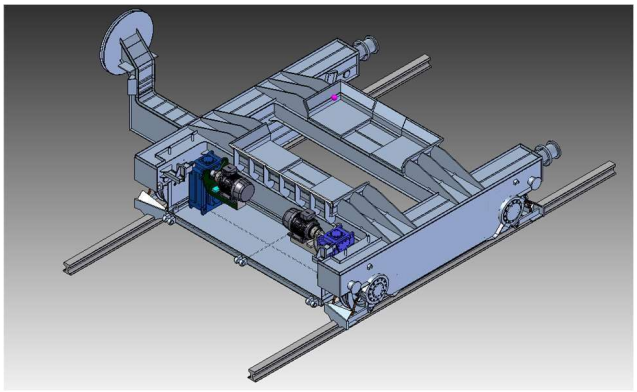

Figure 1.11: Partly dismantled solid-model view showing motor position and connecting frames

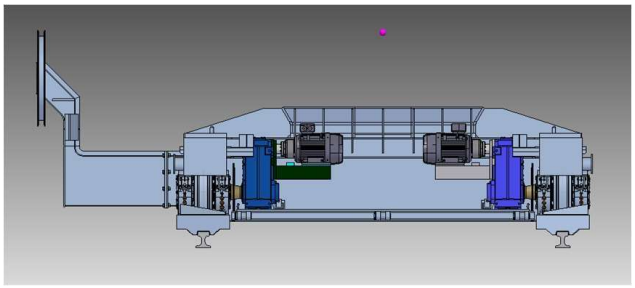

Figure 1.12: Partly dismantled rear view showing motor position and connecting frames

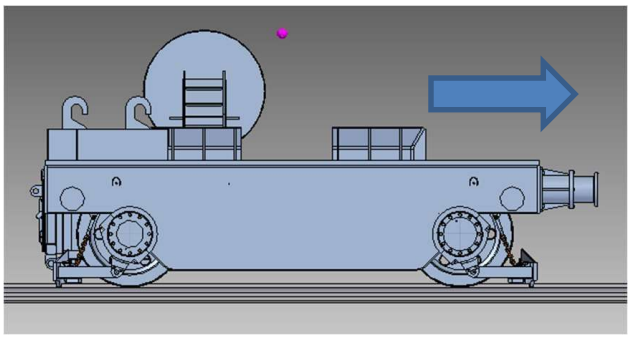

Figure 1.13: Assembled side view of slag-pot car with direction of forward motion indicated by arrow

CHAPTER 2: SYSTEM DESCRIPTION AND FRAME DESIGN BASICS

2.1 System Description

A transfer car of a slag pot is a cost-effective means for safe transport of slag in a steel industry between the loading and unloading points. Figure 2.1 shows a schematic of a transfer car. Its main components are

1. Two identical side frames – one at the left side and one at the right side
2. One connecting frame at the front side
3. One upper and one lower connecting frame at the rear side
4. Two driving wheels at the back side and two driven wheels at the front side
5. Two buffers at the front side
6. One bearing and one shaft or axle for each wheel.
7. One cable arm for the electric power supply.

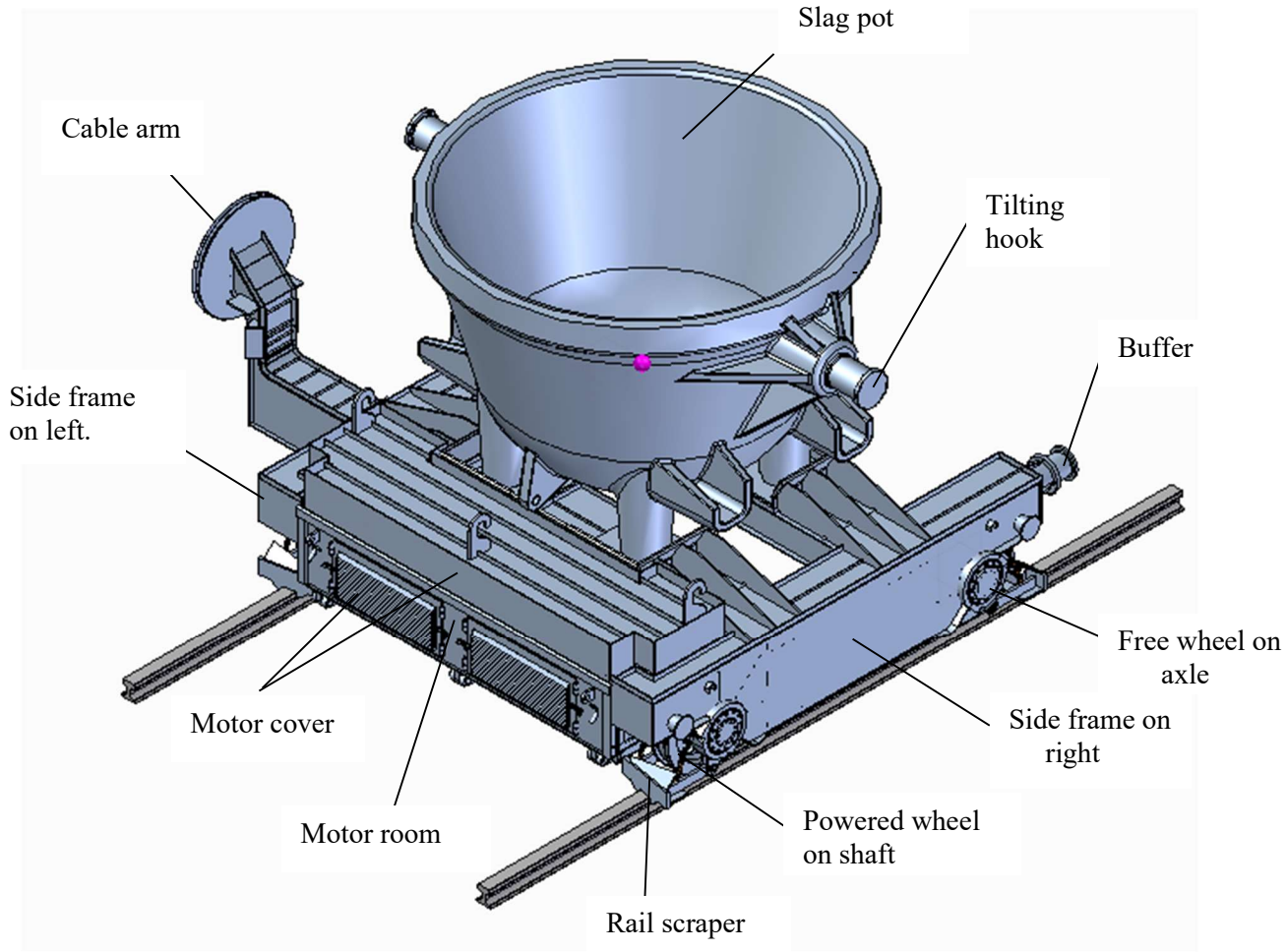

Figure 2.1: A slag pot transfer car and its different components

There are two side frames that together support the connecting frames. At the front side, there is one connecting frame. There are one upper and one lower connecting frame at the back side. The back frames are sturdy welded structures. Under each of the two side frames, two wheels are mounted. In the front side, there is one driving wheel mounted on a shaft transmitting the driving torque from a dedicated plunged-on coaxial gear motor drive. At the back, there is a driven wheel on an axle. Each of the shafts and axles has an anti-friction bearing. By controlling the frequency of the drive, the speed of each shaft could be varied during moving the car along rails on the four wheels. Each drive has a protective cover provided with a maintenance door. On the top sides of the upper back and front connecting frames, there is a pot holder that during the slag loading and transmission holds the slag pot securely with the axis vertical.

There are two tilting hooks with common axis protruding out horizontally from the two sides of the pot. A mechanism mounted on this hook is actuated to unload the slag from the pot by tilting it about the axis. Sturdy rail scrapers and buffers are mounted on the body. The supply lines to the car are clamped to the cable arm which is bolted to the car frame. Most of the frames have been designed by conceiving each as an assembly of a number of rectangular sections. Some related basic theories are mentioned next in this regard.

2.2 Fundamental Design Aspects for Rectangular Sections and their Assembly

Figure 2.2(a) depicts a rectangular section of two orthogonal dimensions b and d parallel to principal axes X and Y passing through the centroid of the area G. For an area of uniform density and thickness, the centres of area, mass and gravity are identical. Only such cases are considered next for composite a body that has members all symmetric about Y axis. Figure 2.2(b) describes such a composite body in the form of a Tee.

It is well known that the second moment of area of a rectangular section about the centroidal axes shown in Figure 2.2 are given by [8]

$$I_{XX} = bd^3/12 \quad \text{and} \quad I_{YY} = db^3/12, \tag{2.1}$$

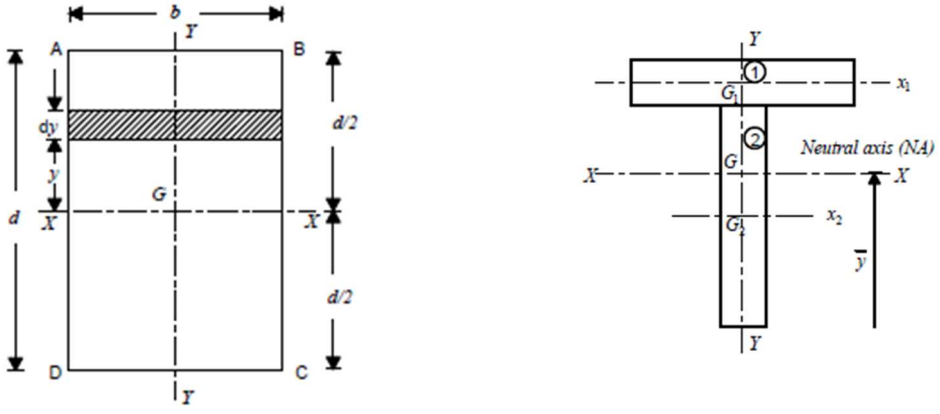

(a) (b)

Figure 2.2: Sections in the form of a (a) rectangle of size $b \times d$ with principal axes XX and YY and (b) Tee beam

along with the expression for the area given as

$A=bd.$ (2.2)

The condition of symmetry for any section like the one shown in Figure 2.3 is written as

$$X_g = x_{g1} = x_{g2} = ... = x_{gi} = 0 .$$ (2.3a)

Of course, the Y coordinate of the centre of mass of such a composite area with is calculated as

$$Y_g = Y_{g1} + \sum_i (A_i y_{gi}) / \sum_i A_i ,$$ (2.3b)

where is y_{gi} is the distance of the centre of Area i at at G_i from the centre of Area 1 located at G_1.

The second moment of area of the composite area about centroidal X axis is obtained by parallel axis theorem as

$$I_{XX} = \sum_i \{ I_{x_{gi}x_{gi}} + A_i (Y_g - Y_{gi})^2 \},$$ (2.4)

where $I \equiv I_{x_{gi}x_{gi}}$, (2.5)

is the centroidal moment of inertia of each area about the respective centroidal axis parallel to X axis.

Figure 2.3 shows another combination of rectangular sections leading to a hollow rectangular section of thicknesses $(b - b_1)/2$ for the horizontal parts and $(d - d_1)/2$ for the vertical parts along with outer boundary ABCD of size $b \times d$. The moment of inertia of the hollow section emerges as

$$I = (bd^3 - b_1 d_1^3)/12 .$$ (2.6)

Besides the centroidal moment of area, the reaction to any member is the other necessary input for finding the bending moment M and stress σ at a distance y from the neutral axis of a member from the well-known equation for bending. The assumptions behind the simple theory are as follows.

1. The beam's substance is uniform and isotropic.
2. The longitudinal fibres of the beam first bend in a straight line with a common Centre of curvature.

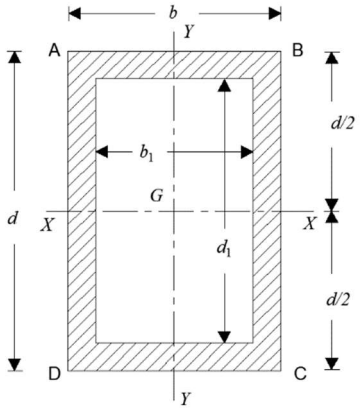

Figure. 2.3 Hollow section of the beam

3. Members are bent toward symmetry and have symmetric cross-sections.
4. The effect of shear is ignored, and the beam is only subjected to pure bending.
5. After bending, plane portions through a beam that are taken normally to the axis of the beamstay plane.
6. Concerning the beam's diameter, the radius of curvature is considerable.

Under the above assumptions, the equation of bending is given by.

$$\frac{\sigma}{y}=\frac{M}{I}=\frac{E}{R_c}, \tag{2.7}$$

where E is the modulus of elasticity and R_c is the radius of curvature of the section.

Of course, the maximum stress occurs at a distance $y_{\max}$ that is furthest from the neutral axis and that stress is estimated from (2.5) as

$$\sigma_{\max} = M/Z, \tag{2.8}$$

where Z represents the section modulus given by

$$Z = I/y_{\max}. \tag{2.9}$$

The bending moment in (2.5) could be obtained by calculating the support reactions by

A) Analytical method

A case of a simply supported beam shown in Figure 2.4 is considered next in the context of these methods.

A) Analytical Method

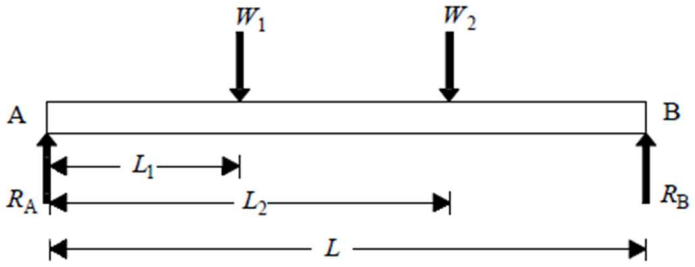

Figure 2.4: A simply supported beam with pointed forces

Figure 2.4 shows a beam AB of length L and is simply supported at the ends A and B. The beam carries two-point loads W_1 and W_2 at a distance L_1 and L_2 from the end A. The equality with zero for both the net vertical forces including support reactions R_A at A and R_B at B along with the net bending moment about A yield

$$R_A + R_B = W_1 + W_2, \tag{2.10a}$$

and $$W_1L_1 + W_2 L_2 - R_B L = 0. \tag{2.10b}$$

Last two equations lead to

$R_B = (W_1 L_1 + W_2 L_2) / L,$ (2.10c)

and $R_A = (W_1 + W_2) - R_B.$ (2.10d)

2.3 Deflection using MACAULAY'S METHOD

This is convenient method for determining the deflections of the beam subjected to the point loads. It mainly consists in the special way the bending moment at any section is expressed and in the way the integrations are carried out [6].

The following rules are observed while using Macaulay's Method:

1. Always take origin on the extreme left of the beam.
2. Take left clockwise moment as positive and left anticlockwise moment as positive.
3. While calculating the slopes and deflections, it is convenient to use the values first in termsof kN and meters.
4. Let consider a simply supported beam AB of length L and carrying a point load W at a distance a from left support and at a distance b from right support is Figure 2.6. The reactions at A and B are given by

   $R_A = Wb/L$ and $R_B = Wa/L$ (2.11)

5. The bending moment at distances a and $(a + b) > x > a$ from A are given respectively by

   $M_C = R_A a = Wab/L,$ (2.12)

   and $M_x = R_A x - W(x-a) = W(bx/L + a - x).$ (2.13)

6. The bending moment at any section is also given by

   $M_x = EI(\mathrm{d}^2 y/\mathrm{d}x^2).$ (2.14)

7. By integrating (2.14) using the no-deflection conditions at the supports A and B and then then using (2.13), the deflection at C is obtained as

   $y_c = -\frac{Wa^2.b^2}{3EIL}.$ (2.15)

With the fundamentals discussed in this chapter, their application in the design of the main frame of the car is discussed in the next section.

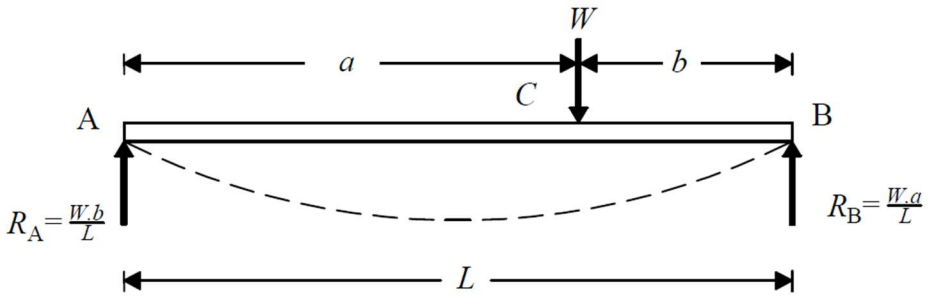

Figure 2.6 Simply supported beam.

CHAPTER 3: DESIGN OF MAIN FRAME

3.1 Design Approach

The design of the main frame has been initiated with the objective of keeping the materials minimum yield stress in any section within the respective limits of E250BR IS2062 and keeping the specification of the centre-to-centre distance of the two rails of the wheel track given as a_t = 4.1m. and wheel to wheel distance as a_w =3000mm, load as per application limits of 100 tons. The point A,B,G and H are the location of slag pot foot.

The distribution of load acting on main frame consists of mass of slag pot (m_P)=30000 kg, and mass of slag (m_S) = 45000 kg.

Therefore, the total mass lies on main frame is *m.*

Where m = m_p + m_s = 75000 kg (3.1)

The configuration of the main frame is selected as depicted in Figure 3.1 for realizing it by welding several frames. These are.

(a) two identical side frames at the left and right side, (1) and (2).
(b) rear lower connecting frame, (3).
(c) rear upper connecting frame, (4).
(d) front connecting frame, (5).

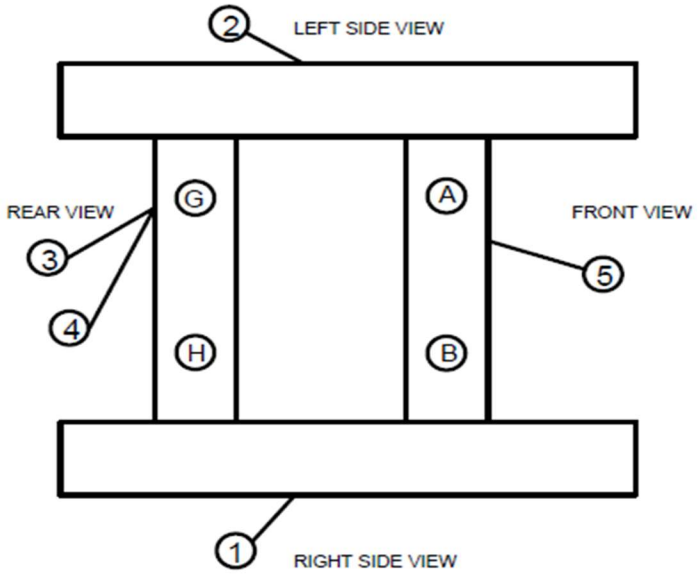

Figure 3.1: Assumed layout of main frame of slag pot transfer car

3.2 Calculation of side frame

Each of the two identical side frames shown in Figure 3.1 is considered as simply supported by a shaft-wheel pair on the left and sides. In Figure 3.6, MN is the simple schematic representation of the beam. At the middle of each frame, half of the load of slag pot acts that is given by

$(W_P+W_S) = W_D$ (3.2)

taken value of g = 9.81 m/s^{2}kg respectively.

Weight of slag pot (W_P) = m_Pg = 294,000N, (3.3)

Weight of slag (W_S) = m_Sg = 441,000N (3.4)

By taking the load factor the total load lies on main frame i.e., W_D

$W_D = mg = 75000\times9.81\times1.34 = 985{,}905$ N (3.5)

A) Predict the cross-section dimension of side frame.

Considering a standard frame material as plain carbon Steel (E250BR) with minimum yield stress Re_H=250MPa[7], using this stress we find out the geometry of the frame keeping length of wheelbase is 3000 mm as our application needs.
After Considering load factor =1.34 and gravity g = 9.81 m/s^2 and one fourth of the total load W_D lies at four point as slag pot foot lies on the main frame. Firstly, foot lies on front and rear connecting frame and these loads distributed on left and right-side frame. i.e., W_D/4

Considering the side frame to achieve the desired cross section of the side frame by taking number of iterations using different variable value of plate thickness *t*, width *b* and height *d* of the cross section as shown in figure 3.2,

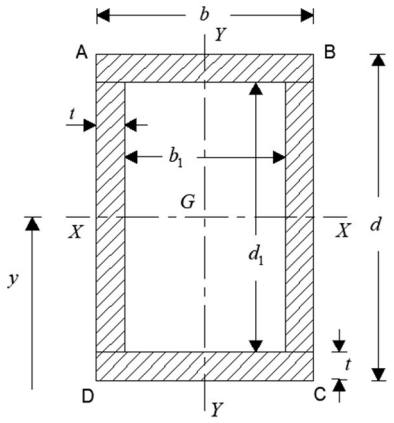

Figure 3.2: Assumed geometry cross-section of the side frame.

Limiting condition: When plate thickness t < 20mm, minimum yield stress R_{eH} = 250 MPa.

- **ITERATION I: Assume t = 5mm, b = 200mm and d = 600mm**

(i) Inertia The moment of inertia of the side frame is obtained with reference to Figure 3.2 as:

$$I_s = [\{200\text{mm} \times (600\text{mm})^3\}/12 - \{190\text{mm} \times (590\text{mm})^3\}/12\}] = 348{,}165{,}833\text{mm}^4 \quad (3.6)$$

(ii) Section of modulus with respective cross section is *Z*.

$$Z = I / y_{max} = 1{,}160{,}552\ \text{mm}^3 \quad (3.7)$$

(iii) Calculation of bending moment assuming the load W_F and W_E act at the two-point F and E on the side frame at a particular distance of point as shown in figure 3.3.

$$W_F = W_E = W_D / 4 = 246{,}476\ \text{N} \quad (3.8)$$

For the calculation of inertia as per assumed limits of yield stress, we need to obtain the bending stress using supports reaction and bending moment of the assume frame. As shown in figure 3.3

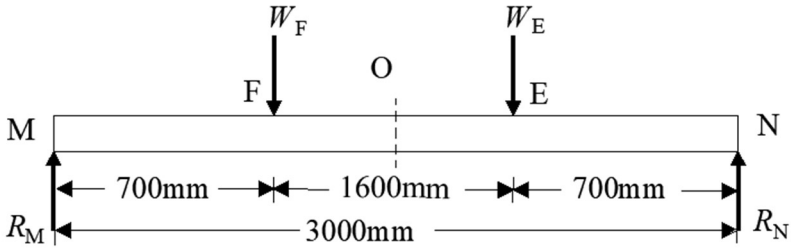

Figure 3.3 A simple schematic of side frame.

Clearly, the end reactions are obtained as

$$R_M = R_N = 246{,}476\ \text{N} \quad (3.9)$$

and the bending moment at the mid span O is obtained as

$$M_O = R_M\, a = 369{,}714{,}000\ \text{N-mm}. \quad (3.10)$$

(iv) Maximum bending stress obtained in the side frame as

$$\sigma_{max} = M/Z \quad = 300 \text{ N/mm}^2 \tag{3.11}$$

Since the bending stress is much higher than the minimum yield stress of the selected plate thickness, width and height of the cross section of frame, the maximum stress developed in it turns out to be much lower than the critical limits. i.e

$$\sigma_{max} > ReH \tag{3.12}$$

$$300 \text{ N/mm}^2 < 250 \text{ N/mm}^2 \tag{3.12a}$$

Here Limiting condion are not satisfied , therefore proceed to next Interation.

- **ITERATION II: Assume t = 10mm, b = 433mm and d = 950mm**

(v) Inertia The moment of inertia of the side frame is obtained with reference to Figure 3.2 as:

$$I_s = [\{433\text{mm} \times (950\text{mm})^3\}/12 - \{413\text{mm} \times (930\text{mm})^3\}/12\}] = 3{,}253{,}167\text{mm}^4 \tag{3.13}$$

(vi) Section of modulus with respective cross section is *Z*.

$$Z = I / y_{\max} = 6{,}849{,}812\text{mm}^3 \tag{3.14}$$

(vii) Maximum bending stress obtained in the side frame keeping bending moment and support reactions keep same as the load acting and wheel to wheel distance is same as shown in figure 3.3.

$$\sigma_{max} = M/Z \quad = 53 \text{ N/mm}^2 \tag{3.15}$$

Since the bending stress is much lower than the yield stress of the selected plate thickness, width and height of the cross section of frame, the maximum bending stress developed much lower than the critical stress limits. i.e

$$\sigma_{max} < R_{eH} \tag{3.16}$$

$$53 \text{ N/mm}^2 < 250 \text{ N/mm}^2 \tag{3.16a}$$

Here Limiting condition are satisfied , therefore selected dimension to be proceeded.

B) Design and prepared model of the side frame

Proceeding over iteration-II side frame is designed with respective value of cross section geometry as shown in figure 3.2.

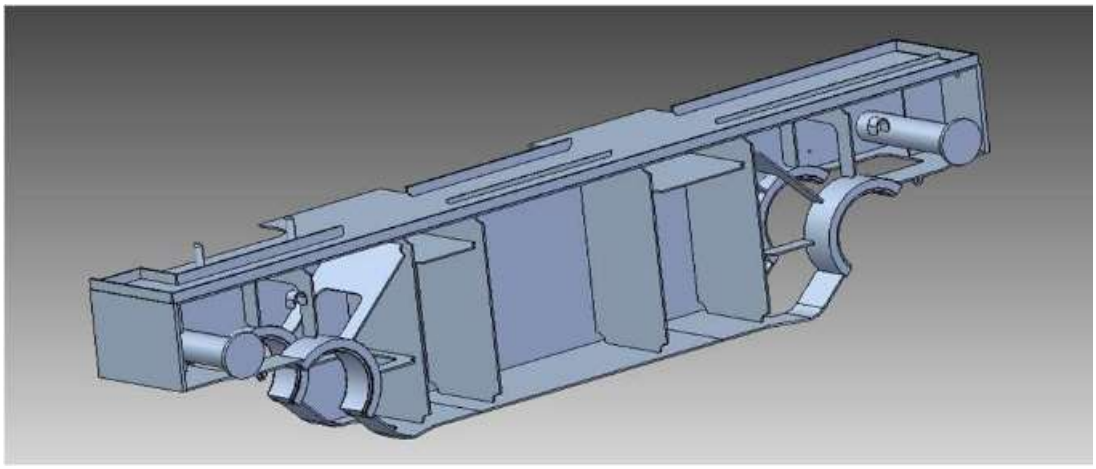

Figure 3.4: 3D model of open section side frame.

3.3 Calculation for connecting rear frame.

Rear frame is combination of two frame one is lower rear connecting frame and other is upper rear connecting frame. It is evident from assumed Figure 3.5 that the lower frame is constituted by vertical members connected with upper horizontal member. Thus, it is symmetric about the mid span and like Tee shape structure for protecting the heat transfer and separation between the motor room and outer side temperature near the converter which has high temperature. Tee member is designed considering to be made up of three hollow boxes as shown in Figure 3.5 containing the hollows labelled as Boxes 3, 4 and 5 taken out of two solid parts marked as Box 1 and 2. Sample calculations based on assumed sizes are provided next.

$$W_D = mg = 75000 \times 9.81 \times 1.34 = 985{,}905 \text{ N} \quad (3.17)$$

A) Predict the cross-section dimension of connecting rear frame.

Considering a standard frame material as plain carbon Steel (E250BR) with minimum yield stress Re_H=250MPa, using this stress we find out the geometry of the frame keeping the centre-to-centre track distance a_t is 4100 mm as per steel plant standard needs.

One fourth of the total load W_D lies at two points on the rear frame also, as slag pot foot lies on the main frame i.e., $W_D/4$

Considering the connecting rear frame to achieve the desired cross section of the side frame by taking number of iterations using different variable value of plate thickness t, width b_1, b_2 and height d_1, d_2 of the cross section as shown in figure 3.5,

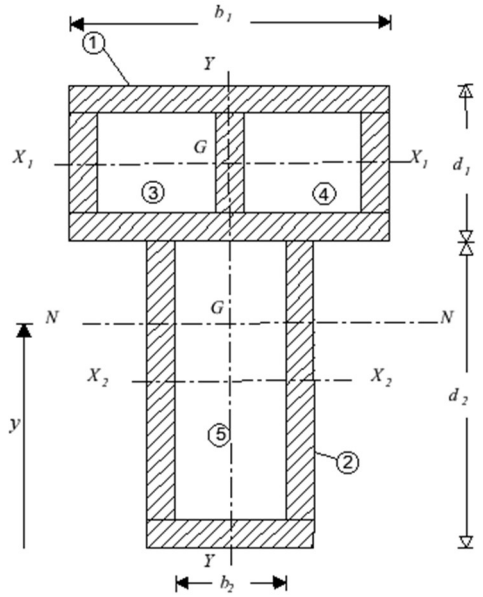

Figure 3.5: Assumed cross-section of the combined rear frame.

Limiting condition: When plate thickness t < 20mm, minimum yield stress R_{eH} = 250 MPa.

- **ITERATION I: Assume t = 5mm, box 1: b_1= 100mm, d_1 = 50mm and box 2: b_2= 50mm, d_2 = 150mm**

(i) The moment of inertia of the side frame is obtained with reference to Figure 3.6 as:

Area of Box 1 in Figure 3.9

$A_1 = 100 \text{ mm} * 50 \text{ mm} = 5000 \text{ mm}^2$ (3.18a)

$y_1 = 50\text{mm}/2 + 150\text{mm} = 175 \text{ mm}$ (3.18b)

Area of Box 2 in Figure 3.9

$A_2 = 50mm * 150mm = 7500\ m\text{m}^2$ (3.19a)

$y_2 = 80mm$ (3.19b)

Distance from the neutral axis to bottom of the frame is found out as

$$y_c = (A_1 y_1 + A_2 y_2)/(A_1 + A_2) = 118 \text{ mm} \quad (3.20)$$

Using parallel axis theorem, the moments of inertia of Box 1 and 2 are respectively obtained as

$$I_1 = 17{,}286{,}666 \text{ mm}^4 \quad (3.20)$$

and $I_2 = 24{,}892{,}500 \text{ mm}^4$. (3.20a)

Hence, the total moment of inertia of the Tee section is found out as

$$I_s = I_1 + I_2 = 42{,}179{,}166 \text{ mm}^4 \quad (3.20b)$$

Areas and centroids of hollow parts indicated as Boxes 3 to 5 in Figure 3.8 are similarly obtained as

$$A_3 = A_4 = 2b_2 d_2 = 2\times 42.5\text{mm}\times 20\text{mm} = 3400 \text{ mm}^2, \quad (3.21a)$$

$$A_5 = b_5 h_5 = 40\text{mm}\times 145\text{mm} = 5800 \text{ mm}^2 \quad (3.21b)$$

$$y_3 = y_4 = 210\text{mm}/2 + 710\text{mm} = 0.365\text{m}, \quad (3.21c)$$

and $y_5 = 80$ m (3.21d)

The total moment of inertia of the hollow boxes is obtained by using parallel axis theorem as

$$I_h = 2I_3 + I_5 = 2(b_3 d_3^2 + A_3 y_3^2) + b_5 d_5^2 + A_5 y_5^2 = 30{,}063{,}883 \text{ mm}^4 \quad (3.22)$$

Hence, the total moment of inertia of the connecting frame is found out as

$$I_n = I_s - I_h = 12{,}115{,}282 \text{ mm}^4 \quad (3.22a)$$

(i) Section of modulus with respective cross section is *Z.*

$$Z = I / y_{max} = 12{,}115{,}282\text{mm}^4 / 118 \text{ mm} = 1{,}026{,}710 \text{ mm}^3 \quad (3.22b)$$

(ii) Calculation of bending moment assuming the load W_G and W_H act at the two-point G and H on the side frame at a particular distance of point as shown in figure 3.6.

$$W_G = W_H = W_D / 4 = 246{,}476 \text{ N} \quad (3.23)$$

For the calculation of inertia as per assumed limits of yield stress, we need to obtain the bending stress using supports reaction and bending moment of the assume frame. As shown in figure 3.6

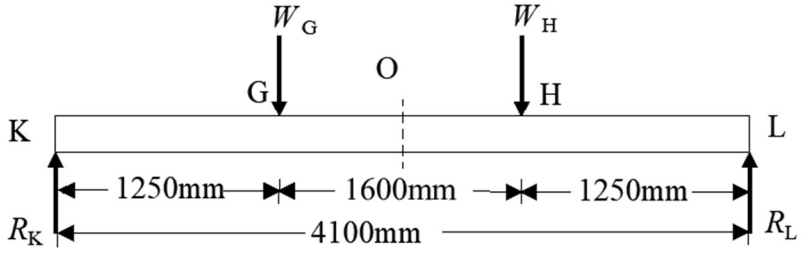

Figure 3.6 A simple schematic of side frame.

Clearly, the end reactions are obtained as

$R_K = R_L = 246{,}476$ N (3.23a)

and the bending moment at the mid span O is obtained as

$M_O = 505{,}275{,}800$ N-mm. (3.23b)

(iii) Maximum bending stress obtained in the side frame as

$$\sigma_{max} = M/Z \quad = 490 \text{ N/mm}^2 \tag{3.24a}$$

Since the bending stress is much higher than the minimum yield stress of the selected plate thickness, width, and height of the cross section of frame, the maximum stress developed in it turns out to be lower than the critical limits. i.e

$$\sigma_{max} > ReH \tag{3.24b}$$

$$490 \text{ N/mm}^2 < 250 \text{ N/mm}^2 \tag{3.24c}$$

Here Limiting condion are not satisfied , therefore proceed to next Interation.

- **ITERATION II: Assume t = 10mm, box 1: b_1= 675mm, d_1 = 230mm and box 2: b_2= 242mm, d_2 = 720mm**

(i) Inertia The moment of inertia of the side frame is obtained with reference to Figure 3.5 as:

Area of Box 1 in Figure 3.9

$A_1 = 230\text{mm} * 675\text{mm} = 155250\ \text{mm}^2$ (3.25)

$y_1 = 230\text{mm}/2 + 720\text{mm} = 835\ \text{mm}$ (3.25a)

Area of Box 2 in Figure 3.9

$A_2 = 242\text{mm} * 720\text{mm} = 174240\ m\text{m}^2$ (3.25b)

$y_2 = 360\ m\text{m}$ (3.25c)

Distance from the neutral axis to bottom of the frame is found out as

$y_c = (A_1 y_1 + A_2 y_2)/(A_1 + A_2) = 584\ \text{mm}$ (3.26)

Using parallel axis theorem, the moments of inertia of Boxes 1 and 2 are respectively obtained as

$I_1 = 1.0465\times10^{10}\ \text{mm}^4$ (3.27)

and $I_2 = 1.6269\times10^{10}\ \text{mm}^4$. (3.27a)

Hence, the total moment of inertia of the Tee section is found out as

$I_s = I_1 + I_2 = 2.6734\times10^{10}\ \text{mm}^4$ (3.27b)

Areas and centroids of hollow parts indicated as Boxes 3 to 5 in Figure 3.5 are similarly obtained as

$A_3 = A_4 = 2b_2 d_2 = 2\times325.5\text{mm}\times210\text{mm} = 136710\ \text{mm}^2$, (3.28)

$A_5 = b_5 h_5 = 226\text{mm}\times710\text{mm} = 160461\ \text{mm}^2$ (3.28a)

$y_3 = y_4 = 210\text{mm}/2+710\text{mm} = 365\ \text{mm}$, (3.28b)

and $y_5 = 10\text{mm}/2+710/2\text{mm} = 365\ \text{mm}$ (3.28c)

The total moment of inertia of the hollow boxes is obtained by using parallel axis theorem as

$I_h = 2I_3 + I_5 = 2(b_3 d_3^2 + A_3 y_3^2) + b_5 d_5^2 + A_5 y_5^2 = 2.3872\times10^{-2}\text{m}^4$ (3.29)

Hence, the total moment of inertia of the connecting frame is found out as

$I_n = I_s - I_h = 0.2862\times10^{10}\ \text{mm}^4$ (3.29a)

(i) Section of modulus with respective cross section is *Z*.

$Z = I / y_{max} = 6{,}849{,}812 mm^3$ (3.30)

(ii) Maximum bending stress obtained in the side frame keeping bending moment and support reactions keep same as the load acting and centre to centre distance of track is same as shown in figure 3.6.

$\sigma_{max} = M/Z$ = 53 N/mm^2 (3.31)

Since the bending stress is much lower than the yield stress of the selected plate thickness, width, and height of the cross section of frame, the maximum bending stress developed much lower than the critical stress limits. i.e

$\sigma_{max} < R_{eH}$ (3.32)

53 N/mm^2 < 250 N/mm^2 (3.32a)

Here Limiting condition are satisfied, therefore selected dimension to be proceeded.

B) Design and prepared model of the rear frame

Proceeding over iteration-II side frame is designed with respective value of cross section geometry.

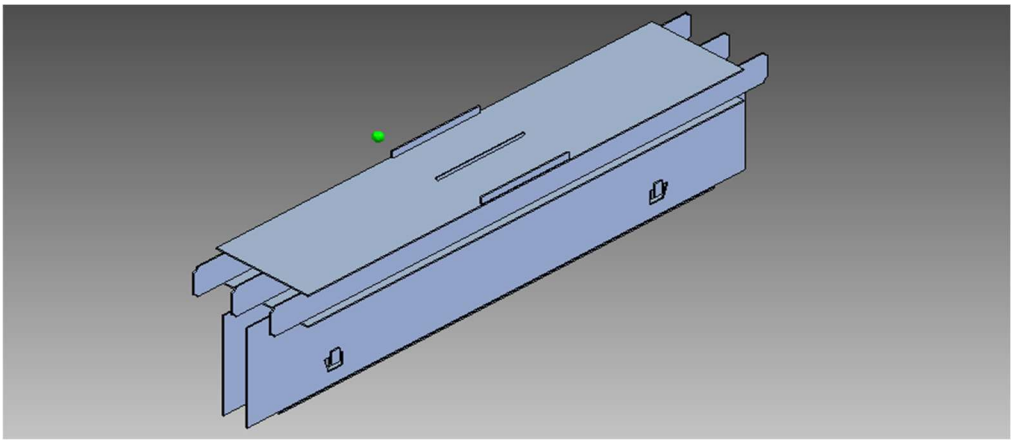

Figure 3.7: 3D model of assembled upper and lower rear connecting frame.

3.4 Calculation for connecting front frame.

It is shown in assumed Figure 3.8 member is designed considering to be made up of two hollow boxes containing the hollows labelled as Boxes 1 and 2 taken out of one solid parts marked as Box $b \times d$, as sample calculations based on assumed sizes are provided next.

$W_D = mg = 75000 \times 9.81 \times 1.34 = 985{,}905$ N

A) Predict the cross-section dimension of connecting front frame.

Considering a standard frame material as plain carbon Steel (E250BR) with minimum yield stress Re_H=250MPa, using this stress we find out the geometry of the frame keeping the centre-to-centre track distance a_t is 4100 mm as per steel plant standard needs.
One fourth of the total load W_D lies at two points on the rear frame also, as slag pot foot lies on the main frame i.e., $W_D/4$

Considering the connecting front connecting frame to achieve the desired cross section of the front frame by taking number of iterations using different variable value of plate thickness t, width b and height d of the cross section as shown in figure 3.8,

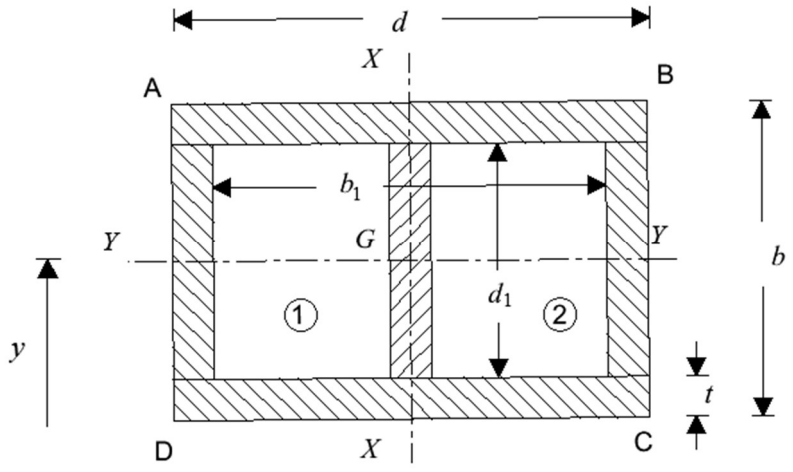

Figure 3.8: Assumed Geometry cross-section of the front frame.

Limiting condition: When plate thickness t < 20mm, minimum yield stress R_{eH} = 250 MPa.

- **ITERATION I: Assume t = 5mm, b = 500mm and d = 200mm**

(i) Inertia The moment of inertia of side frame is obtained with reference to Figure 3.8 as:

$I_s = [\{500\text{mm} \times (200\text{mm})^3\}/12 - \{242.5\text{mm} \times (190\text{mm})^3\}/12\}] = 56{,}115{,}416\text{mm}^4$ (3.33)

(ii) Section of modulus with respective cross section is *Z*.

$Z = I / y_{max} = 561{,}154\ \text{mm}^3$ (3.33a)

(iii) Calculation of bending moment assuming the load W_I and W_J act at the two-point I and J on the front frame at a particular distance of point as shown in figure 3.9.

$W_I = W_J = W_D / 4 = 246{,}476$ N

For the calculation of inertia as per assumed limits of yield stress, we need to obtain the bending stress using supports reaction and bending moment of the assume frame. As shown in figure 3.9

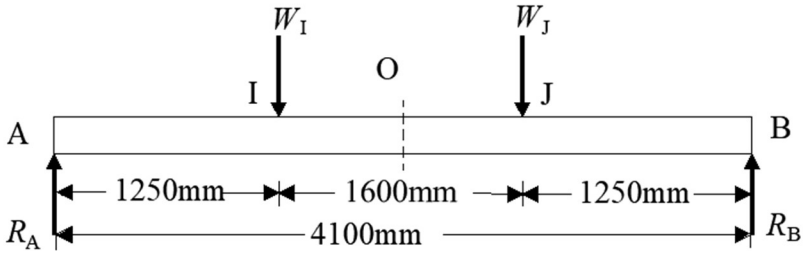

Figure 3.9 A simple schematic of connecting front frame.

Clearly, the end reactions are obtained as

$R_I = R_J = 246{,}476$ N (3.34)

and the bending moment at the mid span O is obtained as

$M_O = 505{,}275{,}800$ N-mm. (3.34a)

(iv) Maximum bending stress obtained in the side frame as

$$\sigma_{max} = M/Z \quad = 900 \text{ N/mm}^2 \tag{3.34b}$$

Since the bending stress is much higher than the minimum yield stress of the selected plate thickness, width, and height of the cross section of frame, the maximum stress developed in it turns out to be much lower than the critical limits. i.e.

$$\sigma_{max} > ReH$$

$$900 \text{ N/mm}^2 < 250 \text{ N/mm}^2 \tag{3.35}$$

Here Limiting conditions are not satisfied , therefore proceed to next Iteration.

- **ITERATION II: Assume t = 10mm, b = 675mm and d = 330mm**

(i) Inertia The moment of inertia of the side frame is obtained with reference to Figure 3.8 as:

$I_s = [\{675\text{mm} \times (330\text{mm})^3\}/12 - 2\{322.5\text{mm} \times (310\text{mm})^3\}/12\}] = 420{,}190{,}000 \text{ mm}^4$

(ii) Section of modulus with respective cross section is *Z.*

$Z = I / y_{\max} = 2{,}246{,}606\text{mm}^3$

(iii) Maximum bending stress obtained in connecting front frame keeping bending moment and support reactions keep same as the load acting and centre to centre track distance is same as shown in figure 3.9.

$$\sigma_{max} = M/Z \quad = 53 \text{ N/mm}^2 \tag{3.38}$$

Since the bending stress is lower than the yield stress of the selected plate thickness, width and height of the cross section of frame, the maximum bending stress developed lower than the critical stress limits. i.e

$$\sigma_{max} < R_{eH}$$

$$198 \text{ N/mm}^2 < 250 \text{ N/mm}^2 \tag{3.39}$$

Here Limiting condition are satisfied, therefore selected dimension to be proceeded.

C) Design and prepared model of connecting front frame.
Proceeding over iteration-II side frame is designed with respective value of cross section geometry.

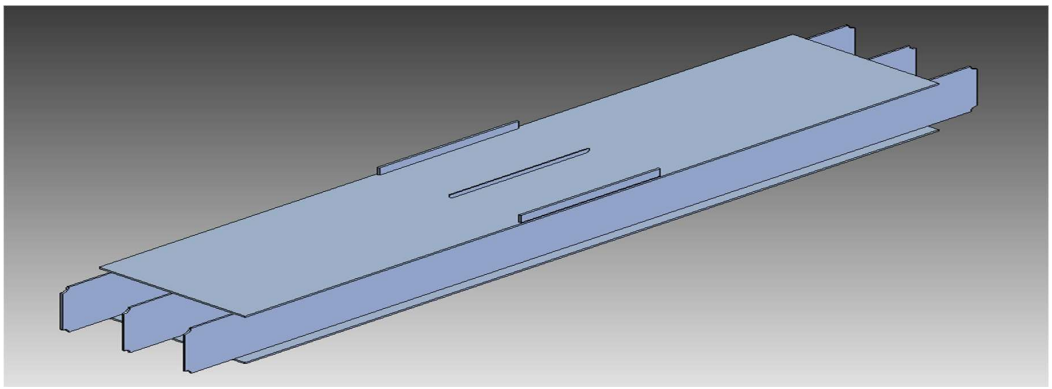

Figure 3.10: 3D model of connecting front frame.

3.5 Maximum Deflection in connecting front frame.

Macaulay method is more convenient method for determining the deflection at section of the beam subjected to point loads. From figure 3.11 it is considered as simply supported beam for simple calculation of deflection at any section of the frame.
The connecting front frame is considered for deflection due to the maximum bending stress approaches near the minimum yield stress. Therefore, the deflection occurs in proposed frame which frame have maximum bending stress reaches near the minimum yield stress limits.
Since, connecting front frame have maximum bending stress near to yield stress.

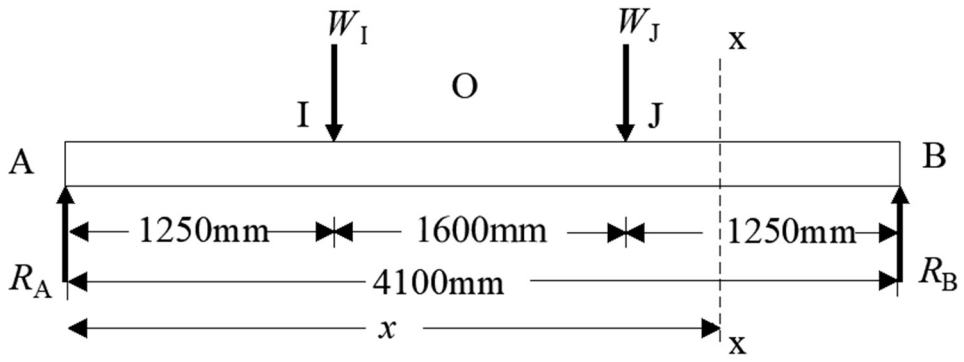

Figure 3.11: Front connecting frame assumed as Simply supported beam.

Using Macaulay Method: -

$$EI\frac{d2y}{dx2} = M_{xx} \tag{3.40}$$

$$M_{xx} = R_1 * x - W_1 * (x - 1.033) - W_2 * (x - 2.633) \tag{3.40a}$$

(i) **Slope equation-**

$$EIy = 251.25 * \frac{x^3}{6} + c1x + c2 \; - 251.25 * \frac{(x-1.033)^3}{6} - 251.25 * \frac{(x-2.633)^3}{6} \tag{3.41}$$

$$c2 = 0 \tag{3.41a}$$

$$c1 = -\,341 \tag{3.42b}$$

Taking,

E =210 Gpa = 210 * 10^3 N/mm^2 = 210 * 10^6 kN/m^2

EI = 38010 kNm^2 (3.43)

(ii) Deflection at point C

$$y_C = \frac{1}{EI}\left[\frac{251.25x^3}{6} + C_1x + C2\right] \tag{3.44}$$

$$y_C = \frac{1}{38010}\left[\frac{251.25*1.033^3}{6} - 341 * 1.033 + 0\right]$$

$$y_C = -0.005\,m\ =\ -5mm$$

(iii) Deflection at point D

$$y_D = \frac{1}{38010}\left[\frac{251.25\ *2.633^3}{6} + (-341 * 1.033) - 251.25\frac{(2.633-1.033)^3}{6}\right]$$

$$y_D = -6\,mm \tag{3.45}$$

(iv) Maximum Deflection occur at distance: -

$$\frac{dy}{dx} = \mathbf{0} \tag{3.46}$$

$$251.25 * \frac{x^2}{2} - 341 - 251.25 * \frac{(x-1.033)^2}{2} = 0$$

$$x = 1887\ \text{mm}$$

Therefore,
Maximum deflection in connecting front frame at x= *1887* mm

$$y_{max} = \frac{1}{EI}\left[\frac{343x^3}{6} + C_1 x - 343\frac{(x-1.033)^3}{6}\right] \tag{3.47}$$

$$y_{max} = -\,8\ \text{mm}$$

3.6 Major sub-member of the main frame.

There are consist of four members of the main frame and by assembling these individuals' member form a complete assembly of the main frame as shown in figure 3.16.

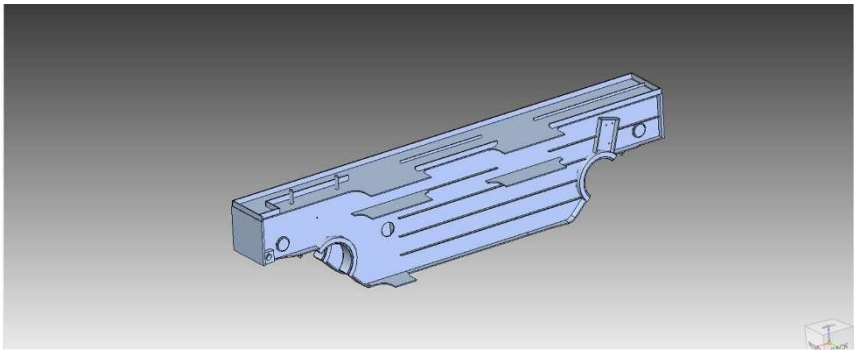

Figure 3.12: Side frame

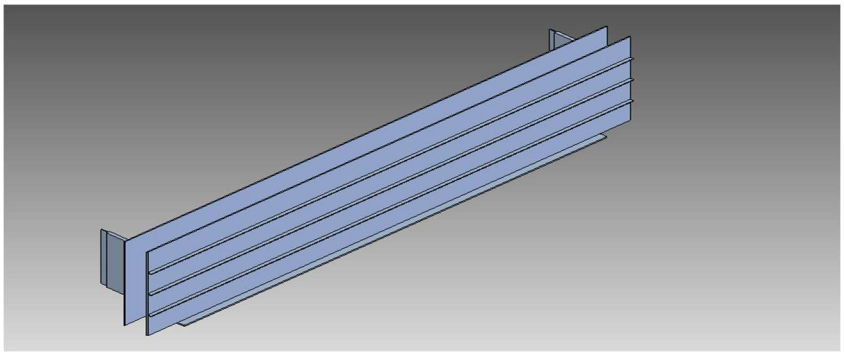

Figure 3.13: Rear lower connecting frame

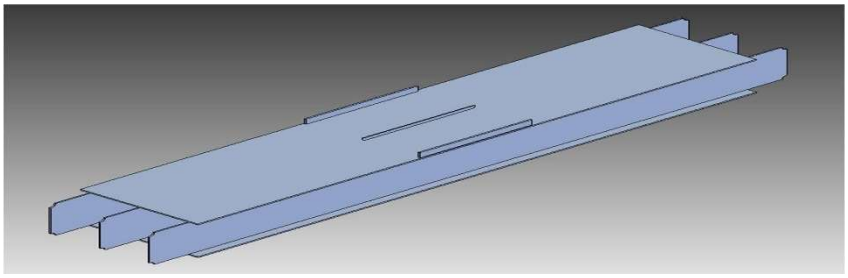

Figure 3.14: Rear upper connecting frame

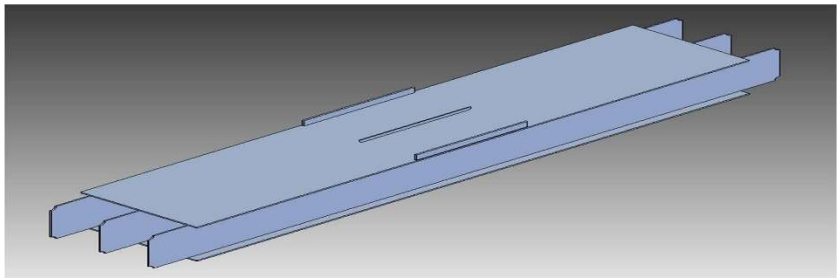

Figure 3.15: Front connecting frame

3.6 Major sub-members of the main frame.

The configuration of the main frame is selected as depicted in Figure 3.16 for realizing it by welding several frames as shown below.

(a) two identical side frames at the left and right side, as shown in Figure 3.12
(b) rear lower connecting frame, as shown in Figure 3.13
(c) rear upper connecting frame, as shown in Figure 3.14
(d) front connecting frame, as shown in Figure 3.15.

Starting from a set of assumed sizes for the components, the subsequent calculation for each member involves the determination of moment of inertia of the respective section along the identification of the location with respect to the end supports and the value of both the maximum stress and the deflection.

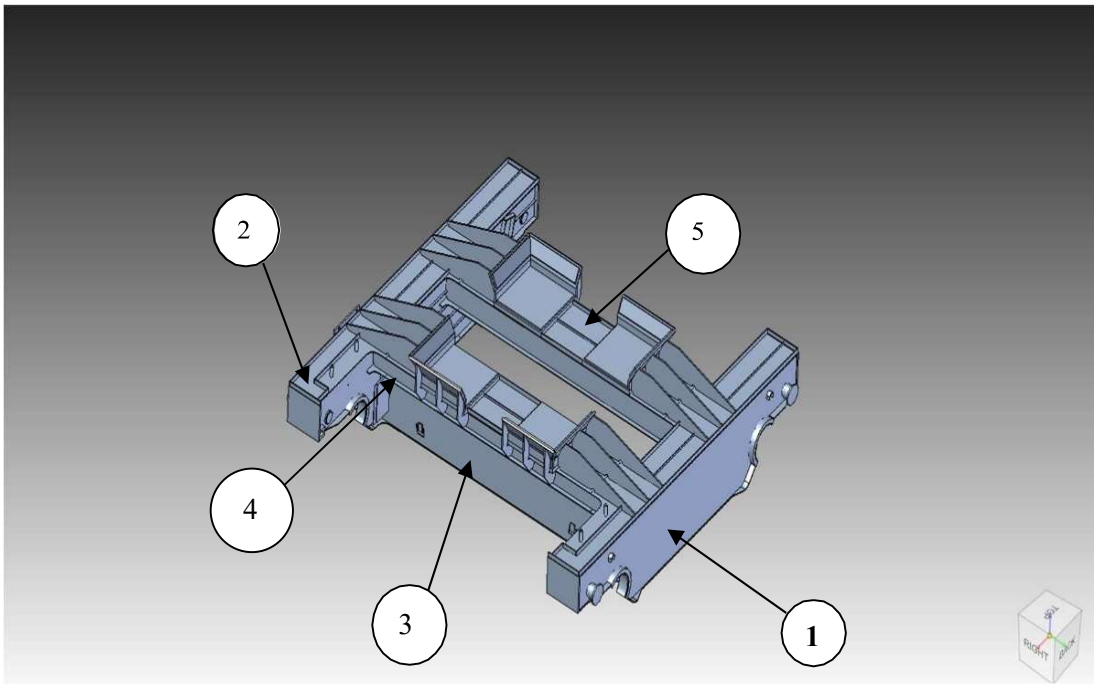

Figure 3.16: Frame assembly schematic of a slag pot – 1, 2: Side frames, 3, 4: Back-side lower and upper connecting frame, 5: Front-side upper connecting frames respectively.

CHAPTER 4: STANDARD ITEMS & STABILITY OF CAR

4.1 Standard Items

Design by selection in this section involves.

a) Wheel
b) Bearing
c) Buffer

4.2 Wheel

A) Parameters of design:

a) Carrying capacity of ladle and speed of transfer car.
b) Installed block design of axle box units and of drive.
c) Possible installation of weight measuring system
d) Rakes for cleaning the way between rails.
e) Furnished with argon blowing system for hot steel having the quick removable connection of argon duct with teeming ladle.
f) Thermal insulation of drive and electric equipment mechanisms

B) Vehicle specification

Dead weight of car = 25 ton
Carrying capacity = 100 ton
Wheel speed = 30 m/min
Number of wheels = 4

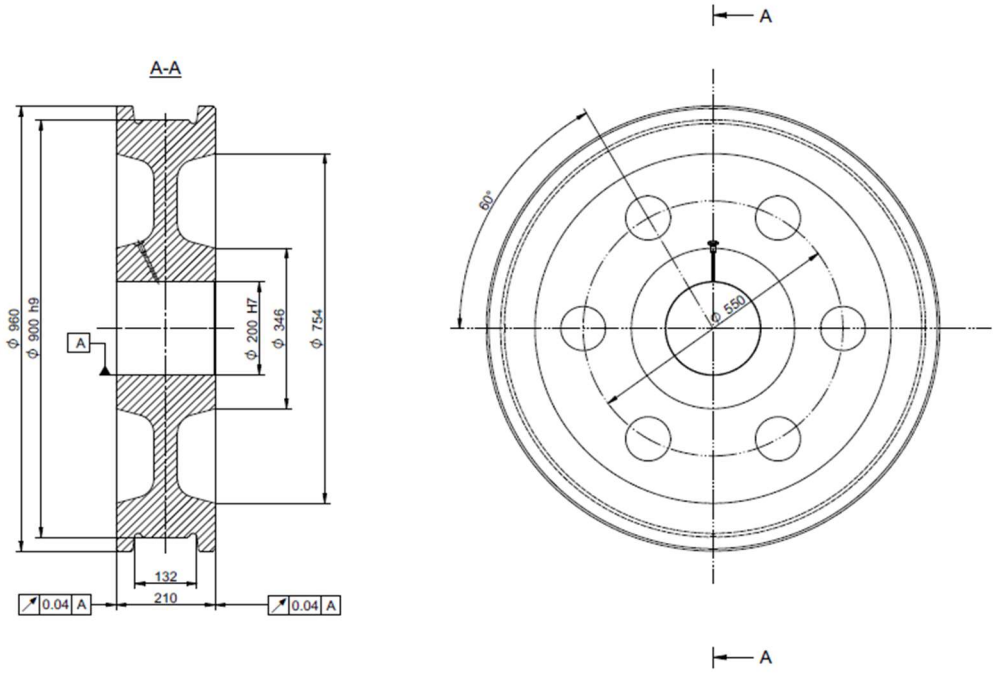

Figure 4.1: Geometry of wheel

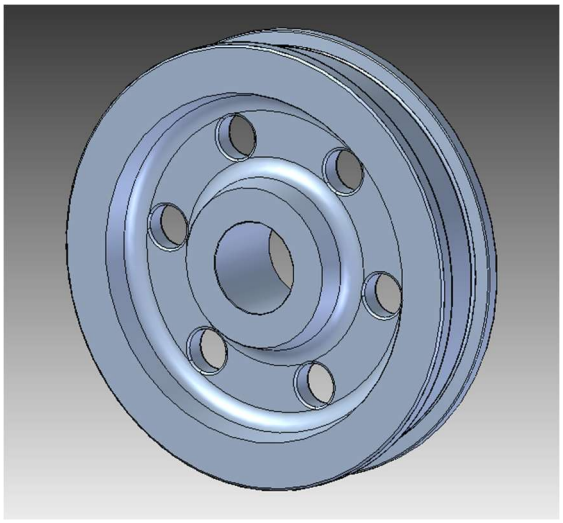

Fig. 4.2 3D Model of Wheel

Materials

A) Cast steel, 42CrMo4, DIN 15093

- **Chemical Composition**: It is a chromium-molybdenum alloy steel with the following composition:

a) Chromium (Cr): 0.38-0.45%
b) Molybdenum (Mo): 0.15-0.30%
c) Carbon ©: 0.38-0.45%
d) Silicon (Si): 0.40%
e) Manganese (Mn): 0.60-0.90%
f) Phosphorus (P): ≤0.035%
g) Sulfur (S): ≤0.035%

- **Hardenability:** It has medium good hardenability and is suitable for hot applications up to 500°C.

B) DIN 15 093 Crane Wheels:

- These crane wheels are used for driven and non-driven wheel sets.
- Material options include:

a) GE420 (GS-70)
b) G42CrMo4+QT (GS-42CrMo4V)
c) 42CrMo4+QT (42CrMo4V) drop forged.

- **42CrMo5-04**:

a) Quenched and tempered to 850-1000 N/mm² or higher.
b) Tread and inner wheel flanges non-slip hardened to HRc 48-54 (hardening depth min. 10 mm)[2].

C) 42CrMo4 Strength:

a) **Tensile Strength** ≥ 1080 Mpa.
b) Yield Strength ≥ 930 Mpa.
c) Elongation ≥ 12%
d) Brinell Hardness ≥ 229 (for annealed or high-temperature steel rod.)
e) Hardness: After quenching and tempering, the hardness is approximately 30-35 HRC (Rockwell C scale).
f) Fatigue Strength: Good fatigue resistance due to its alloy composition

In summary, 42CrMo4 is a versatile steel alloy, and DIN 15 093 crane wheels are used in various applications, with material options including 42CrMo4+QT.

D) Design of wheel:

Stress concentration of wheel is major factor for designing of wheel. **Stress concentration**: **stress raisers** are a location in an object where stress is concentrated. An object is strongest when force is evenly distributed over its area, so a reduction in area, e.g., caused by a crack, results in a localized increase in stress. A material can fail, via a propagating crack, when a concentrated stress exceeds the material's theoretical cohesive strength. The real fracture strength of a material is always lower than the theoretical value because most materials contain small cracks or contaminants (especially foreign particles) that concentrate stress.

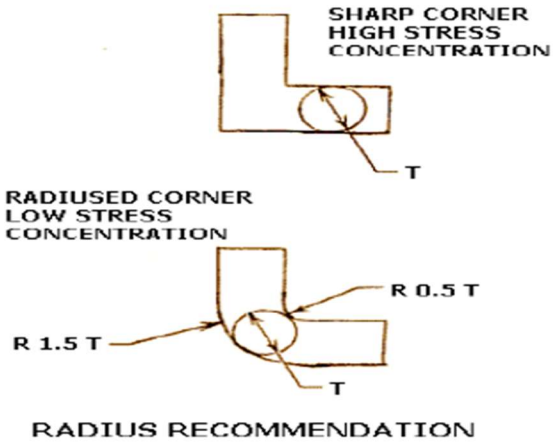

Figure 4.3 Stress concentration [2]

E) Methods of reducing stress concentration

Several methods are available to reduce stress concentration in machine parts. Some of them are as follows:

(i) Provide a fillet radius so that the cross-section may change gradually.
(ii) Sometimes an elliptical fillet is also used.
(iii) If a notch is unavoidable, it is better to provide a number of small notches rather than a long one. This reduces the stress concentration to a large extent.
(iv) If a projection is unavoidable from design considerations it is preferable to provide a narrow notch than a wide notch.
(v) Stress relieving groove are sometimes provided.

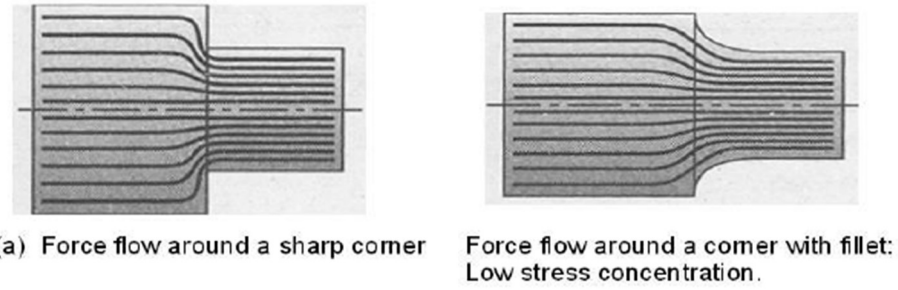

Fig.4.4 stress flow lines in sharp corner.[2]

4.3 Selection of Bearing

A) Spherical roller bearing with relubrication features (22330 CC/W33):

Spherical roller bearings can accommodate heavy loads in both directions. They are self-aligning and accommodate misalignment and shaft deflections, with virtually no increase in friction or temperature. The design includes features to facilitate relubrication. The bearings can be used in a modular system, including housings, sleeves, and nuts.

(i) Accommodate misalignment.
(ii) High load carrying capacity.
(iii) Relubrication features.
(iv) Low friction and long service life
(v) Increased wear resistance

Figure 2.5: 3D model of bearing [5]

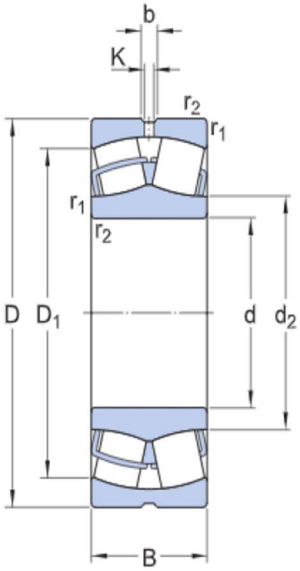

Figure 2.6: Geometry of bearing [5]

Dimensions

Bore diameter	150 mm.
Outside diameter	320 mm.
Width	108 mm.

Performance

Basic dynamic load rating	1539 kN
Basic static load rating	1760 kN
Reference speed	1600 r/min
Limiting speed	2000 r/min

Dimensions

d	150 mm	Bore diameter
D	320 mm	Outside diameter
B	108 mm	Width
d_2	≈ 188 mm	Shoulder diameter of inner ring
D_1	≈ 266 mm	Shoulder/recess diameter of outer ring
b	16.7 mm	Width of lubrication groove
K	9 mm	Diameter of lubrication hole
$r_{1,2}$	min. 4 mm	Chamfer dimension

4.4 Stability of slag pot transfer car

A) Load distribution on four wheels of the Slag pot transfer car

Force acting on a four-wheel vehicle at rest, we can form three independent equations to take care of four unknown viz., four reactions at the wheels. Thus, the problem is simplified by the considering it as a two-wheel car, i.e. the reaction on the both rear wheels is equal and also on both front wheels.

Let the R_A and R_B be the vertical reactions at rear and front wheel respectively.

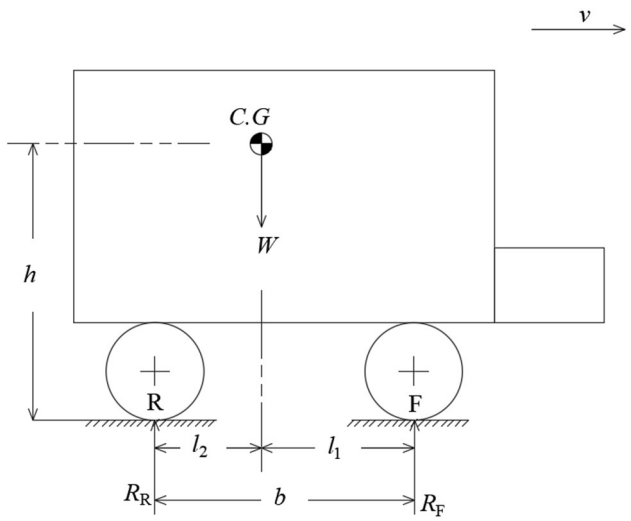

Figure.4.7: Block diagram of car at rest

Where

W = weight of the wheel

b = wheelbase

l_1 = distance of CG from the front axle.

h = height of CG from the road surface

a = wheel track

R_F = Vertical reaction at front wheel

R_R = Vertical reaction at rear wheel

Sum of vertical reactions at front and rear wheel.

$$\sum V = 0 \tag{4.1}$$

$$W = R_A + R_B \tag{4.2}$$

Sum of moment about front wheel F

$$\sum M_F = 0 \tag{4.3}$$

$$Wl = R_R b \tag{4.3a}$$

Reaction force at rear wheel

$$R_R = \frac{Wl}{b} \quad (4.4)$$

Reaction force at front wheel

$$R_F = W(1 - \frac{l}{b}) \quad (4.4a)$$

4.5 Stability of Slag pot transfer car after collision.

D'Alembert's principle:

D'Alembert's principle generalizes the principle of virtual work from static to dynamical systems by introducing forces of inertia which, when added to the applied forces in a system, result in dynamic equilibrium. D'Alembert's principle can be applied in cases of kinematic constraints that depend on velocities.

$$\sum_i (F_i - m_i a_i) = 0 \quad (4.5)$$

Here,

F_i is the total applied force on the i th spot.

i is the integral used to identify the variable relating to the particular particle in the system.

m_i denotes the mass of the particle at the ith place.

a_i denotes the acceleration of the particle.

r_i denotes the virtual displacement of the ith particle.

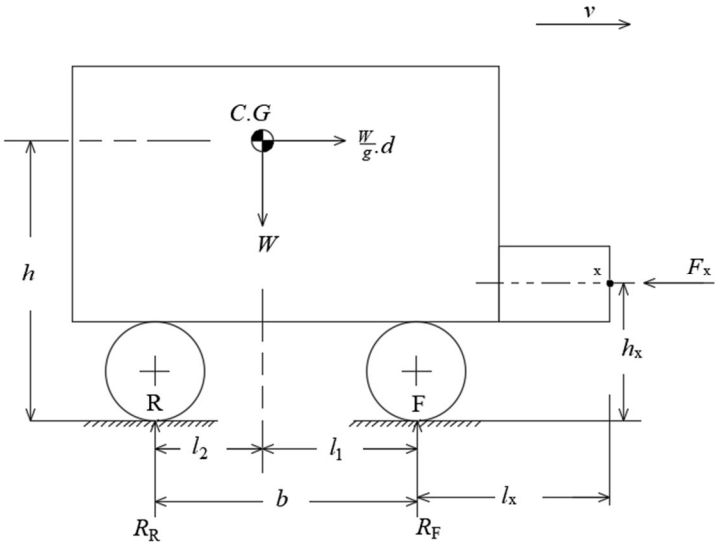

Fig.2.3 Block diagram of slag pot transfer car.

Car tends to be toppled about front wheel B & buffer will try to compress to it maximum deflection.
Vehicle will not topple suddenly about buffer point x because car have slag pot weight, slag weight and its own weight. i.e., 100 ton.

Where,
V is the velocity of car in x-direction and deacceleration *(d= −a)*
F_x is Spring force (buffer).
F_x= k.s
Therefore,
Taking moment about point B,

$$\sum M_B = 0 \tag{4.6}$$

$$\frac{W}{g}.d.h + R_A.L - W.L_2 - F_x.h_x = 0$$

$$R_A = \frac{1}{L}.[(W.L_2 + F_x.h_x) - (\frac{W}{g}.d.h)] \tag{4.6a}$$

Term I: $(W.L_2 + F_x.h_x)$ (4.7)
Term II: $(\frac{W}{g}.d.h)$ (4.7a)
Therefore, for positive value of R_A the term I should always greater than term II
Hence, Limiting condition for stability of slag pot transfer car:

$$(W.L_2 + F_x.h_x) \geq (\frac{W}{g}.d.h) \tag{4.8}$$

Case I. Stable condition

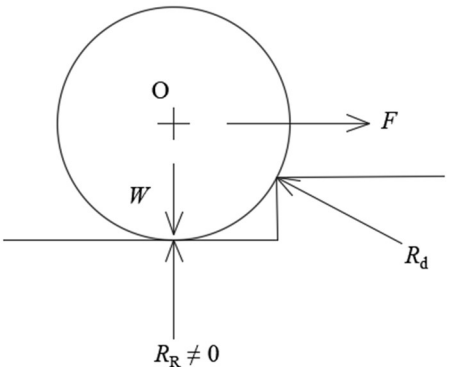

Case II. Unstable condition

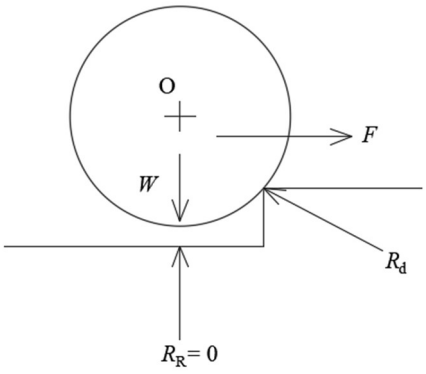

Figure 2.4. Free body diagram of rear wheel of the slag pot transfer car

Therefore, we can say that for stability the value of R_A should always be $R_A > 0$.
For stable R_A have some positive value $R_A \neq 0$. When the wheel lifted about point contact then the reaction (R_A) acting on wheel will be $R_A = 0$ and car will topple.

CHAPTER 5: ANALYSIS WITH RESULT AND DISCUSSION

5.1 General Description of FEM Calculation Method

The load assumptions are determined by the ISO EN 13001 in terms of static strength. As per EN13001 the loads are divided into Main Loads, Special Loads. The classification depends on the frequency of occurrence of these loads will occur and how big their impact and consequences are.
Using NX2212 advance simulation version is used to perform this analysis.

5.2 Load Cases on the frame

LC		Description	Fx [kN]	Fy [kN]	Fz [kN]
1	Gr	Dead load of slag pot car			
		m=20t			-196.2
2	Gsp	Dead load of full slag pot			
		m=80t			-784.8
3	Fy1	Collision load on support console, transverse to rails			
		0.25 x Gsp = 20t		196.2	
4	Fx1	Collision load on support console, longitudinal to rails			
		0.25 x Gsp = 20t	196.2		
5	Fz1	Collision load on support console, in vertical direction			
		0.30 x Gsp = 24t			-235.4
6	S1	Frame distortion due to uneven rails on left front side			
		3.0 mm --> 1‰ of wheel distance 3000 mm			
7	S2	Frame distortion due to uneven rails on left rear side			
		3.0 mm --> 1‰ of wheel distance 3000 mm			
8	Pu	Buffer impact (buffer stroke = 100mm and velocity = 30m/min)			
		Deceleration = 1.25 m/s^2	100.0		
9	Nz	Emergency pull with full slag pot (asymmetric)			
		Pull force = 147kN (Nz=100t x g x 0.15)	147.2		
10	Ah	Lifting of empty slag pot car			
		m = Gr			-196.2

Table.5.1: Load cases

5.3 Boundary Condition

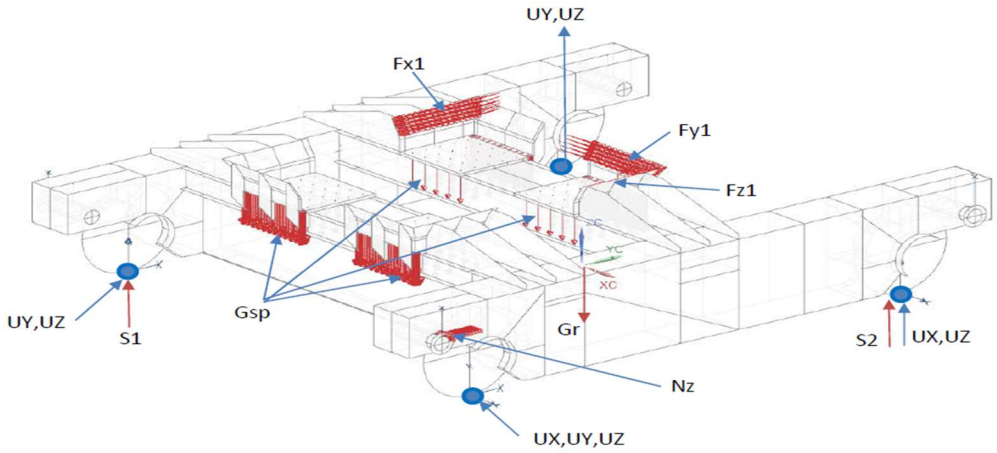

(a)

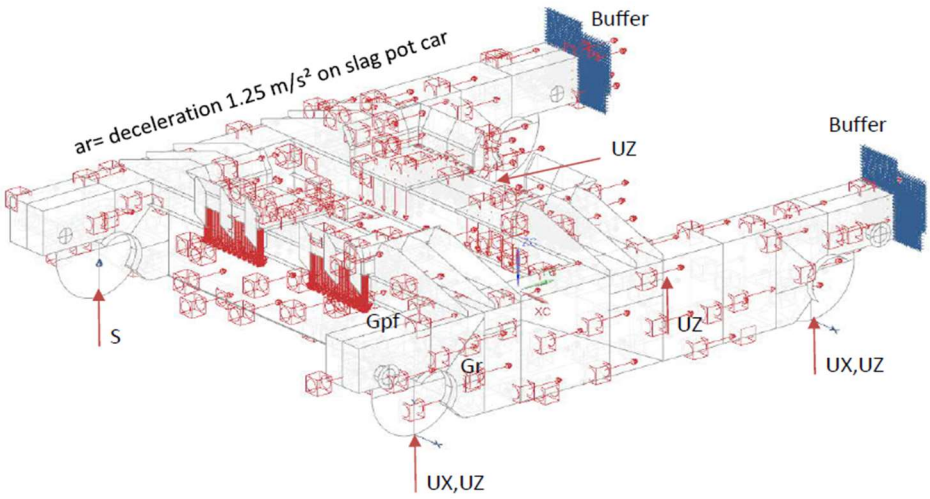

(b)

Figure 5.1: Boundary condition of the main frame

5.4 Static Stress Evaluation of the main frame

A) When Plate thickness: t ≤ 20 mm

Material:	E250 BR
Yield point: fy	250 N/mm²
General resistance factor of the plate: γ_m	1.1
Specific resistance factor of the plate: γ_{sm}	1
Limit design stress: fRd	**227 N/mm²**

Load case	Von-Mises Stress			Remarks
LCC	TOP	BOTTOM		
01	15.8 N/mm²	17.0 N/mm²	< zul 227 N/mm²	
02	167.6 N/mm²	147.8 N/mm²	< zul 227 N/mm²	
03	156.9 N/mm²	141.3 N/mm²	< zul 227 N/mm²	
04	156.9 N/mm²	141.3 N/mm²	< zul 227 N/mm²	
05	169.5 N/mm²	151.3 N/mm²	< zul 227 N/mm²	
06	169.5 N/mm²	151.3 N/mm²	< zul 227 N/mm²	
11	206.8 N/mm²	180.5 N/mm²	< zul 227 N/mm²	
12	209.3 N/mm²	213.0 N/mm²	< zul 227 N/mm²	
13	183.3 N/mm²	204.6 N/mm²	< zul 227 N/mm²	
14	76.8 N/mm²	62.5 N/mm²	< zul 227 N/mm²	
15	156.5 N/mm²	141.8 N/mm²	< zul 227 N/mm²	
16	156.5 N/mm²	141.8 N/mm²	< zul 227 N/mm²	
17	203.0 N/mm²	209.6 N/mm²	< zul 227 N/mm²	
18	139.4 N/mm²	138.0 N/mm²	< zul 227 N/mm²	

Table.5.2: List of variable load results for t≤20mm

B) When Plate thickness: 20 mm < t ≤ 40 mm

Material:	E250 BR
Yield point: fy	240 N/mm²
General resistance factor of the plate: γ_m	1.1
Specific resistance factor of the plate: γ_{sm}	1
Limit design stress: fRd	**218 N/mm²**

Load case	Von-Mises Stress			Remarks
LCC	TOP	BOTTOM		
01	5.5 N/mm²	6.1 N/mm²	< zul 218 N/mm²	
02	55.0 N/mm²	54.5 N/mm²	< zul 218 N/mm²	
03	56.3 N/mm²	55.6 N/mm²	< zul 218 N/mm²	
04	56.3 N/mm²	55.6 N/mm²	< zul 218 N/mm²	
05	60.4 N/mm²	59.5 N/mm²	< zul 218 N/mm²	
06	60.4 N/mm²	59.5 N/mm²	< zul 218 N/mm²	
11	67.6 N/mm²	67.3 N/mm²	< zul 218 N/mm²	
12	193.3 N/mm²	200.5 N/mm²	< zul 218 N/mm²	
13	63.3 N/mm²	71.9 N/mm²	< zul 218 N/mm²	
14	51.5 N/mm²	62.5 N/mm²	< zul 218 N/mm²	
15	57.4 N/mm²	55.6 N/mm²	< zul 218 N/mm²	
16	57.4 N/mm²	55.6 N/mm²	< zul 218 N/mm²	

Table.5.3: List of variable load results for 20≤ t ≤ 40mm

A) When Plate thickness: 40 mm < t ≤ 100 mm

Material:	E250 BR
Yield point: fy	230 N/mm²
General resistance factor of the plate: γ_m	1.1
Specific resistance factor of the plate: γ_{sm}	1
Limit design stress: fRd	**209 N/mm²**

Load case	Von-Mises Stress			Remarks
LCC	TOP	BOTTOM		
01	5.5 N/mm²	6.1 N/mm²	< zul 209 N/mm²	
02	69.6 N/mm²	53.5 N/mm²	< zul 209 N/mm²	
03	65.9 N/mm²	50.6 N/mm²	< zul 209 N/mm²	
04	38.3 N/mm²	40.8 N/mm²	< zul 209 N/mm²	
05	71.1 N/mm²	54.2 N/mm²	< zul 209 N/mm²	
06	41.2 N/mm²	44.1 N/mm²	< zul 209 N/mm²	
11	85.9 N/mm²	65.3 N/mm²	< zul 209 N/mm²	
12	117.5 N/mm²	139.6 N/mm²	< zul 209 N/mm²	
13	63.3 N/mm²	71.9 N/mm²	< zul 209 N/mm²	
14	51.2 N/mm²	54.4 N/mm²	< zul 209 N/mm²	
15	50.8 N/mm²	65.7 N/mm²	< zul 209 N/mm²	
16	65.7 N/mm²	50.8 N/mm²	< zul 209 N/mm²	
17	73.8 N/mm²	77.3 N/mm²	< zul 209 N/mm²	
18	27.9 N/mm²	22.6 N/mm²	< zul 209 N/mm²	

Table.5.3: List of variable load results for 40≤ t≤100mm

5.5 Graphical Representation of Deformation

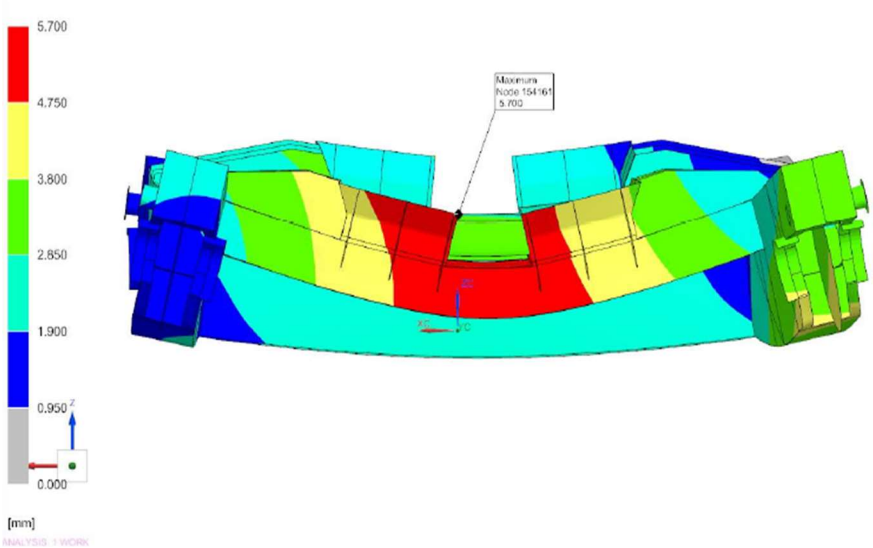

Figure 5.2 Deformation under LCC 02 – 1 x Gr + 1.2 x Gsp

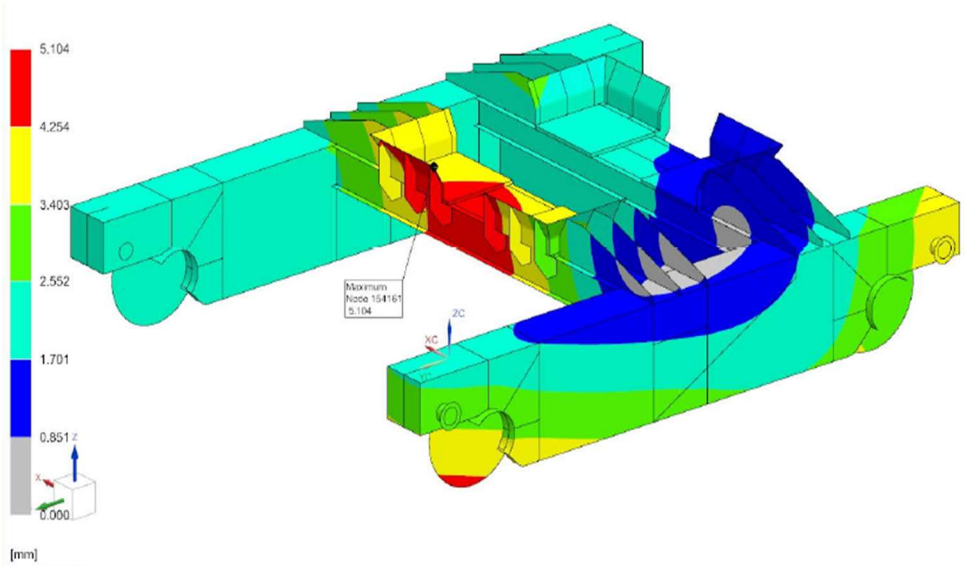

Figure 5.3: Deformation under LCC 05 – 1 x Gr + 1.2 x Gsp + S1*

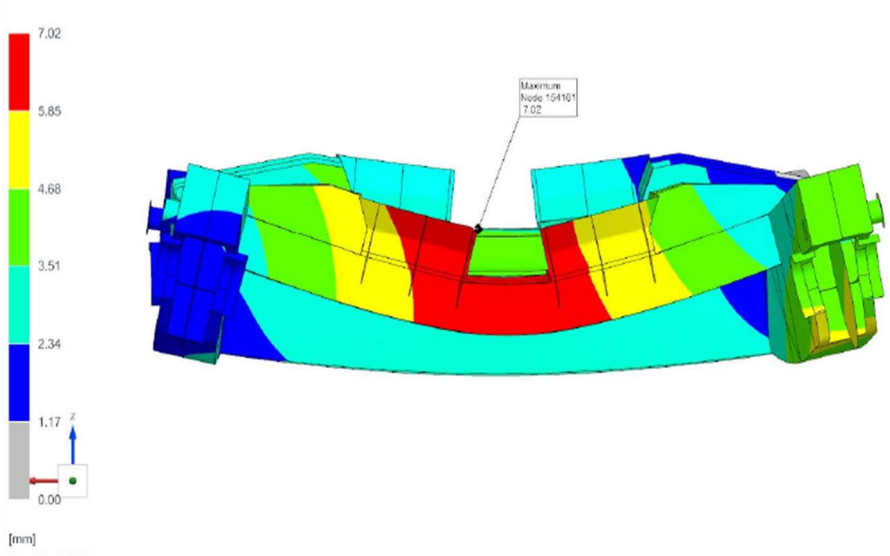

Figure 5.4: Deformation under LCC 11 – 1 x Gr + 1.5 x Gsp

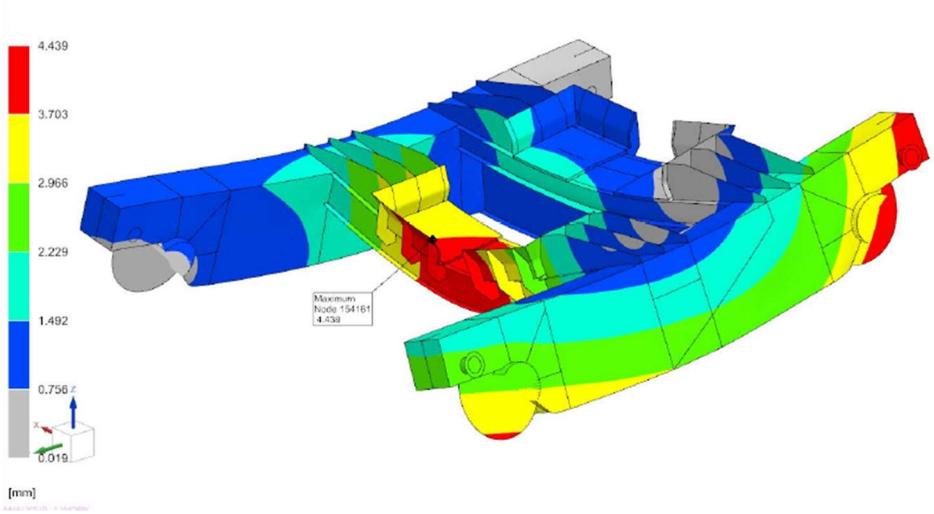

Figure 5.5: Deformation under LCC 15 – 1.1 x Gr + 1.1 x Gsp + Pu + S1*

5.6 Graphical Representation of Stress

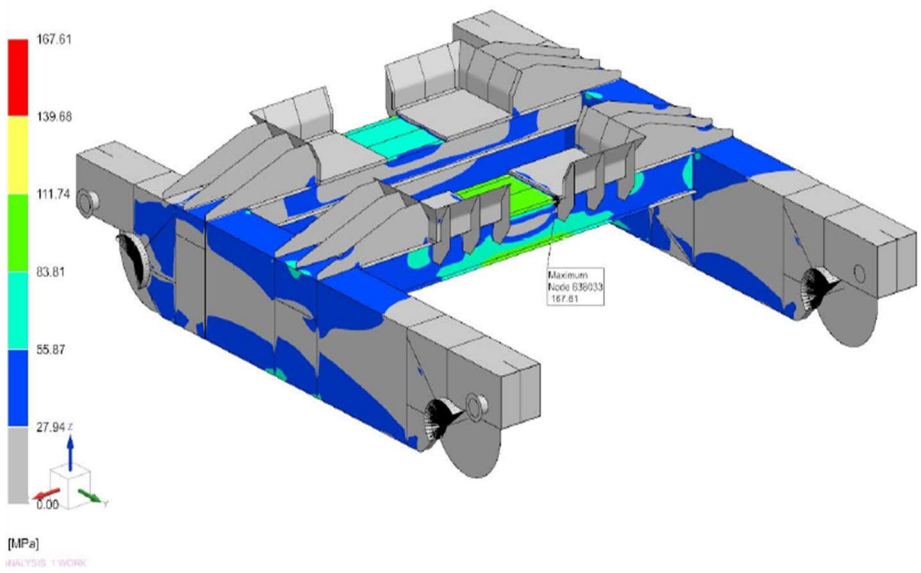

Figure 5.5: Top Reference Stresses (Von Mises) under all Main Loads LCC 02

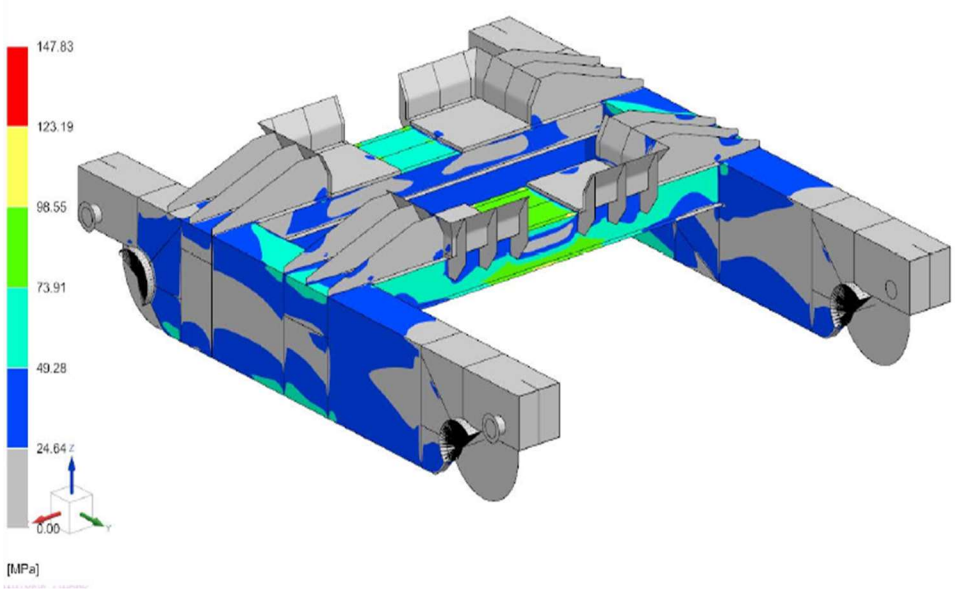

Figure 5.6: Bottom Reference Stresses (Von Mises) under all Main Loads LCC 02

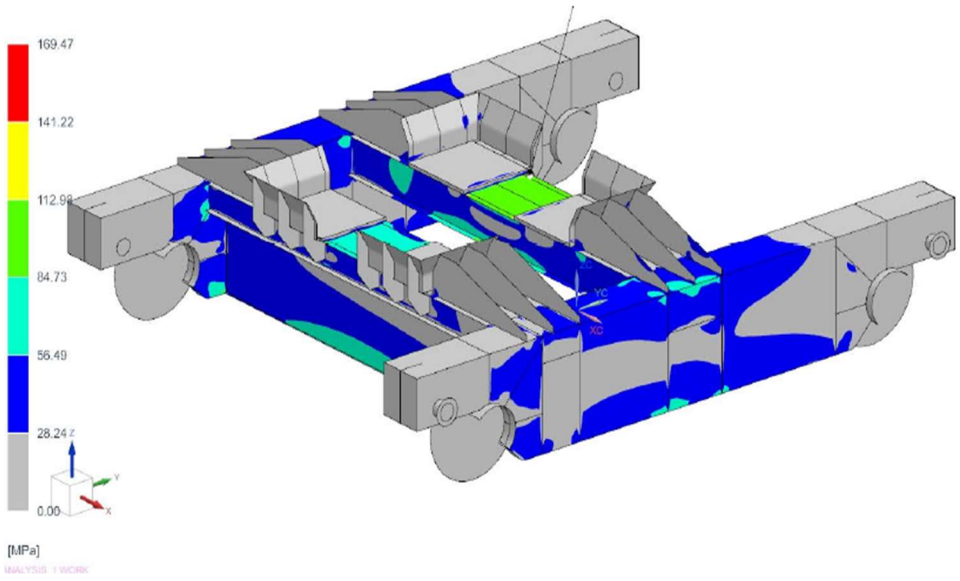

Figure 5.7: Top Reference Stresses (Von Mises) under all Main Loads LCC 05

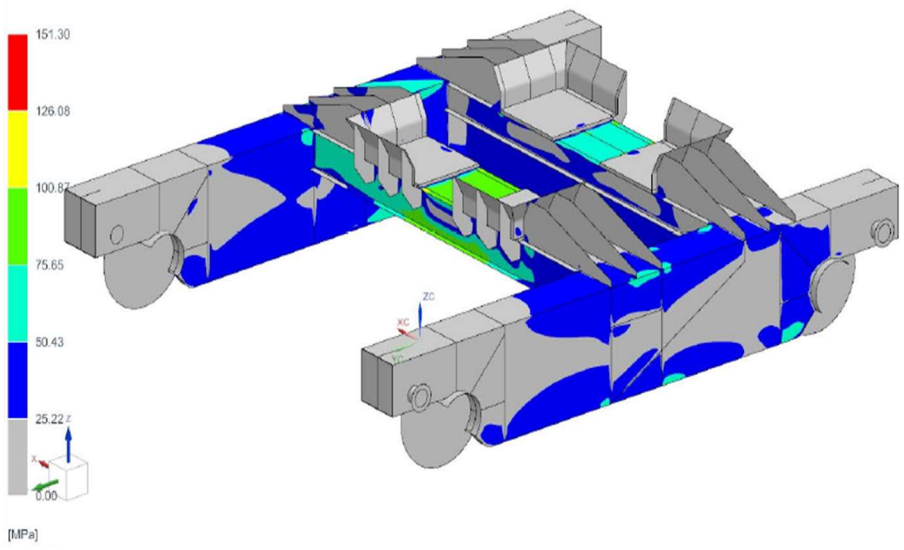

Figure 5.8: Bottom Reference Stresses (Von Mises) under all Main Loads LCC 05

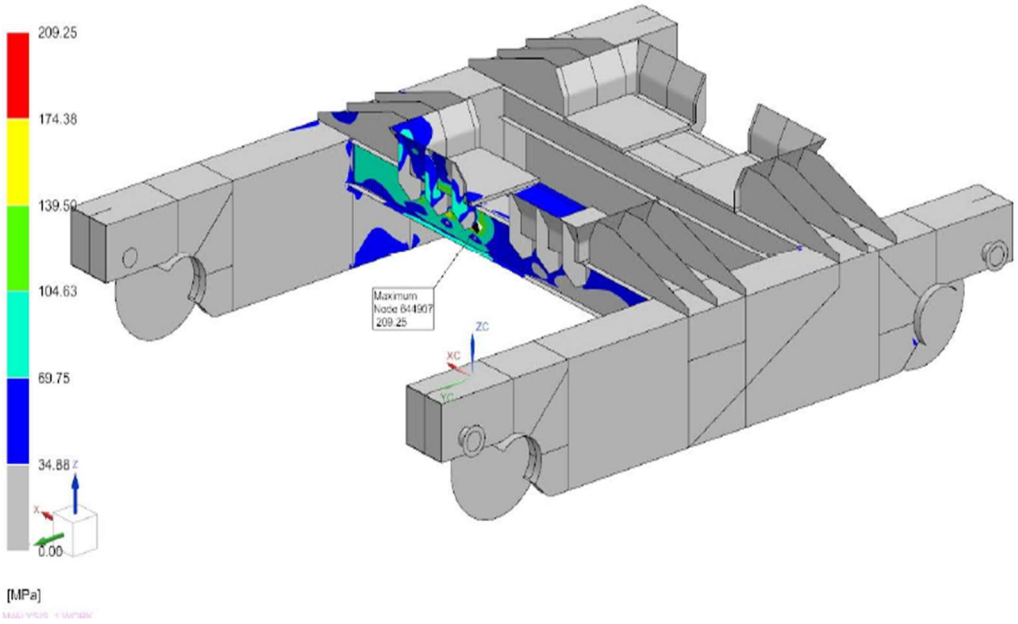

Figure 5.9: Top Reference Stresses (Von Mises) under all Special Loads LCC 12

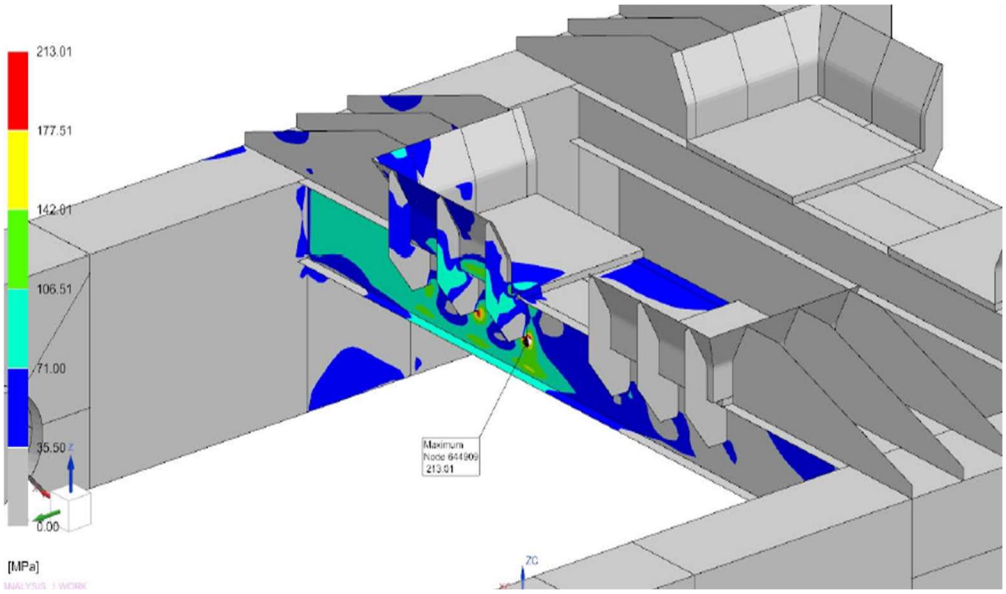

Figure 5.10: Bottom Reference Stresses (Von Mises) under all Special Loads LCC 12

Result and Discussion

As per EN-13001, the static stresses in a welded steel structure, which occur during normal operation as well as under all feasible extra-ordinary loading conditions, have to be lower than the permissible stresses given by the code.

Following the standard, it has to be distinguished between normal operational loads (main loads - load category A), extra-ordinary loads (special loads - load category C), which among others cover particular supporting conditions or rarely occurring loading situations. These load categories are mentioned as Main Loads (A) and Special Loads (C).

Furthermore, in the standard different permissible stresses are specified for the un-welded material and for welded regions respectively. Additionally, the permissible stresses for the welded regions depend on type and quality of the welding as well as on the local acting stress conditions (tensile, compressive, shear or reference stresses).

The slag pot transfer car mainly is built up with plates in steel quality E250BR, IS:2062.
In this calculation the load factors according EN 13001 were considered. The safety factor of material amounts 1.1.

It has to be noted, however, that EN-standard 13001 strictly considered is valid for an evaluation of stress results, which are obtained by analytical calculations (method of nominal stresses).

As already mentioned, the load factors are already included in the load (Material 1.1). If the stresses are calculated by a more accurate method such as by the finite element method (FEM), even higher permissible stresses can be taken into consideration. A fundamental pre-condition for the acceptance of higher stresses is that they result from local stress concentrations, and they are confined to single model nodes. Within the Main Loads local stresses up to the yield strength are permissible and within the special loads also local stresses above the yield strength are permissible.

Summary

The model for the slag pot transfer car primarily is built up by shell elements and contains all relevant kinematic functions and connections. With these models all relevant loads (like weight loads, car movements) and load case combinations were calculated.
In a first step the static loads were calculated. Under Operating Loads (=Main Loads) and special loads all global stresses remain within the valid stress limits.
Therefore, it can be stated that the slag transfer car is well designed.

CHAPTER 6: CONCLUSION AND FUTURE SCOPE

6.1 Conclusion

The new design frame for the slag pot transfer car appears to be a significant improvement over the previous model. Several key conclusions can be drawn based on its features and potential benefits:

Enhanced Durability: The new design likely incorporates materials and structural reinforcements to enhance durability, ensuring longevity even in demanding industrial environments where slag transfer occurs.

Improved Safety Features: Safety is paramount in industrial settings. The new design likely integrates advanced safety features such as reinforced barriers, emergency brakes, and possibly even automation to minimize the risk of accidents during slag transfer operations.

Increased Efficiency: Efficiency gains are often a primary driver for redesigning industrial equipment. The new frame design likely optimizes the arrangement of components, possibly reducing weight, improving movability, and streamlining the slag transfer process for increased productivity.

Cost-Effectiveness: While initial investment in a new design may be significant, over time, the cost-effectiveness of the new frame can be realized through reduced maintenance requirements, decreased downtime, and improved operational efficiency.

Environmental Considerations: Depending on the specific modifications, the new design may also address environmental concerns by reducing emissions, improving energy efficiency, or incorporating sustainable materials.

Overall, the new design frame for the slag pot transfer car promises to deliver a range of benefits, including enhanced durability, improved safety, increased efficiency, cost-effectiveness, and potentially positive environmental impacts. These factors collectively contribute to its potential to positively impact operations within industrial settings where slag handling is a critical aspect of production processes.

6.2 Future Scope of slag pot transfer car in steel plants.

The future scope of new design slag pot transfer cars could be quite promising, considering advancements in materials, automation, and sustainability. Here are some potential areas of development and their implications:

Material Innovation: Research into new materials or composites could lead to lighter yet stronger slag pot transfer cars, reducing energy consumption and improving efficiency. Materials that are more resistant to corrosion and wear could also prolong the lifespan of these vehicles.

Automation and Robotics: Integration of advanced automation and robotics technology could enhance the efficiency and safety of slag pot transfer operations. Automated systems for loading and unloading slag pots, as well as autonomous navigation, could streamline processes and reduce the need for manual labour.

Data Analytics and Predictive Maintenance: Implementation of sensors and data analytics software could enable predictive maintenance of slag pot transfer cars. By monitoring various parameters such as temperature, vibration, and wear, maintenance activities can be scheduled proactively, minimizing downtime and maximizing operational efficiency.

Environmental Considerations: Future designs may prioritize environmental sustainability by incorporating features such as energy-efficient propulsion systems, emissions reduction technologies, and recycling capabilities for slag and other waste materials. This aligns with the growing focus on sustainability and reducing the environmental footprint of industrial operations.

Integration with Smart Factory Concepts: Slag pot transfer cars could be integrated into broader smart factory concepts, enabling seamless communication and coordination with other equipment and systems. This could improve overall production efficiency and flexibility, allowing for adaptive manufacturing processes.

Customization and Modular Design: Future slag pot transfer cars may feature modular designs that allow for easier customization to suit specific application requirements. This flexibility could accommodate diverse industrial settings and evolving operational needs.

Safety Enhancements: Continuous improvement in safety features, such as collision avoidance systems, emergency braking mechanisms, and advanced warning systems, can further enhance workplace safety and reduce the risk of accidents.

Overall, the future scope of new design slag pot transfer cars lies in leveraging technological advancements to improve efficiency, safety, and sustainability in industrial operations. Collaboration between industry stakeholders, researchers, and technology providers will be key to realizing these advancements and driving innovation in this field.

REFERENCES

1. Ministry of steel association,2024, Designed, National Information Centre (NIC).
2. Atul,Lalit kumar,Bijendra Singh,2016,Design of Wheel of a Ladle Car in a Steel Manufacturing Industry,International Journal of all research education and scientific methods,P1-8.
3. Old image of existing slag pot transfer car https://model-shop.ee/en/freight-cars/slag-car-46144.html.
4. Manual operated slag pot transfer car Alamy Limited https://www.alamy.de/ web design, stock photography.
5. Dr. R K BANSAL,2008, Engineering mechanics, Laxmi publication ltd. P296-300,105-110.,531-535.
6. RS Khurmi and N Khurmi,2002, Strength of materials. Laxmi publication.P101-104
7. The Bureau of Indian Standards, 1990, Indian Standard of Steels,General metallurgical sectional Committee.
8. Naga Sudha, V., Raghuram, K.S., Savitri, V., Shanthi Swaroopini, A. (2020), Design Optimization of Slag Pot Transfer Car, Naga Sudha, V., Raghuram, K.S., Savitri, V., Shanthi Swaroopini, A. (2020). Design Optimization of Slag Pot Transfer Car,269-270.
9. Bearing catalogue www.skf.com/skf/product catalogue.
10. Thomas D.Gillespie,(1992),Fundamentals of vehicles Dynamics ,SAE publications Group, Society of Automotive engineers, ,P310.